M. Sc. Thesis

by

Nazlı Ataç

A Thesis Submitted to the

Graduate School of Health Sciences

in Partial Fullfilment of the Requirements for

the Degree of

Master of Science

in

Medical Physiology

Koc University

August 25, 2014

Koc University

Graduate School of Health Sciences

This is to certify that I have examined this copy of a master's thesis by

Nazlı Ataç

and have found that it is complete and satisfactory in all respects,

and that any and all revisions required by the final

examining committee have been made.

Committee Members:

Dr. Özlem Yalçın (Advisor)

Assoc. Prof. Kerem Pekkan

Assoc. Prof. Yusuf Özgür Çakmak

Date: August, 18th 2014

SHEAR INDUCED DAMAGE OF ERYTHROCYTES ASSESSED BY THE DECREASE OF THEIR DEFORMABILITY

ABSTRACT

Background: Mechanical damage or hemolysis in some cases, followed by exposure to high shear stress (≥100 Pa) was recorded in the previous studies. On the contrary, applying shear stress at physiological levels (5-20 Pa, 300 sec) was recently proved to improve erythrocyte deformability. This study aimed to analyze the erythrocyte deformability under shear stress exposure and to determine a breakpoint between improving and impairing erythrocyte deformability (i.e. Subhemolytic threshold). Our second goal was to examine the influence of frequency of intermittent shear stress exposure on subhemolytic threshold. Thirdly, two models of damage were involved in this study to observe how the subhemolytic threshold shifted when erythrocyte deformability was manipulated externally.

Methods: Various levels of shear stress (0-100) were applied to erythrocytes samples for 300 seconds. Couette type shearing system was used for shear stress exposure and deformability was immediately measured following the shear stress via ektacytometry. Application time of shear exposure was varied although the total exposure time was kept constant: Measurements involved repeating either 30 seconds of shear exposure 10 times (10 x 30 sec) or 15 seconds of exposure 20 times (20 x 15 sec). Erythrocyte deformability was manipulated by two models: Oxidative damage by 1 mM of hydrogen peroxide and metabolic depletion.

Results: 5 to 10 donors were involved in the study for each model of the study. The subhemolytic damage with constant shear stress was recorded in between 30-40 Pa for the donors. Intermittent shear exposure resulted in improved deformability for more frequent applications at physiological shear stress range. Exposure of erythrocytes to supraphysiological levels of shear, on the other hand, revealed erythrocyte damage both for continuous and intermittent shear stress. Erythrocyte damage models resulted in impaired deformability for oxidative damage model, while metabolic depletion model showed slight increase. Free hemoglobin amount was checked in order to see whether hemolysis was present or not.

Conclusion: Biphasic response was observed for the effect of shear stress on erythrocyte mechanical properties. Duration and rate of shear application had a minor influence on subhemolytic threshold compared to the magnitude of application. External modifications were used and altered deformability and subhemolytic threshold was obtained.

ÖZETÇE

Geçmiş: Önceki mevcut çalışmalarda yüksek kayma geriliminin (≥100 Pa) kan hasarı veya hemolize neden olduğu saptanmıştır. Bunun yanı sıra, fizyolojik değerlerde uygulanan kayma geriliminin eritrosit deformabilitesini iyileştirdiği bilinmektedir (5-20 Pa). Bu çalışmadaki temel amaç eritrosit deformabilitesindeki artış ve bozulma arasındaki eşik değerini saptamak olmuştur (Subhemolitik hasar). Çalışmanın ikincil amacı ise aralıklı uygulanan kayma gerilimi sıklığının subhemolitik hasar eşiğinde herhangi bir değişikliğe yol açıp açmadığının saptanması yönünde olmuştur. Son olarak, eritrosit deformabilitesi çeşitli modeller ile modifiye edilmiş subhemolitik eşik açısından önemi araştırılmıştır.

Yöntemler: Eritrosit örneklerine 0-100 Pa aralığında 300 saniye boyunca kayma gerilimi uygulanmıştır. Couette tipi bir ektasitometri yöntemi ile kayma gerilimi uygulanmış ve hemen ardından deformabilite ölçülmüştür. Kayma gerilimi süresi değişkenlik gösterip toplam uygulama süresi sabit tutulmuştur: Ölçümler 30 saniye boyunca 10 defa (10 x 30 s) veya 15 saniye boyunca 20 defa olmak üzere değişkenlik göstermiştir. Eritrosit deformabilitesini modifiye etmek için iki model kullanılmıştır: 1 mM hidrojen peroksit ile oksidatif hasar modeli ve metabolik deplesyon.

Bulgular: Her deney seti için çalışmaya 5-10 kişi dahil edilmiştir. Subhemolitik hasar eşiği 30-40 Pa aralığında saptanmıştır. Aralıklı kayma gerilimi uygulamasının eritrosit deformabilitesi üzerindeki artışı fizyolojik değerler içinde daha sık uygulandığında görülmüştür. Fizyolojik değerlerin aşılması kayma geriliminin sürekli veya aralıklı olması fark gözetmeksizin eritrositler üzerinde hasara yol açmıştır. Eritrosit hasarını tetikleyici modeller eritrosit deformabilitesi hidrojen peroksit muamelesi için düşüş gösterirken metabolik deplesyon deneyinde bir miktar artış saptanmıştır. Süspansiyon ortamındaki serbest hemoglobin miktarı analiz edilerek ortamdaki hemolizin varlığı kontrol edilmiştir.

Sonuç: Kayma geriliminin eritrosit mekaniğine etkisinde bifazik bir ilişki saptanmıştır. Kayma geriliminin sıklık ve süresi subhemolitik eşiğin saptanmasında minör bir etkiye sahip olup kayma geriliminin büyüklüğü daha büyük miktarda etkili olmuştur. Eritrosit mekaniğini değiştirmek adına çeşitli modeller kuıllanılmış ve eritrosit deformabilitesi ve subhemolitik hasar eşiğinde değişiklik gözlenmiştir.

ACKNOWLEDGEMENTS

There is no other word to begin but express my grief for Prof. Oğuz Kerim Başkurt, my advisor, for his unexpected death in July 2013. Sometimes two years are more than enough for a person to learn what life exactly is.

I would like to thank;

Firstly to Prof. Başkurt as I saw a true example of how to stand for every word, both academically and personally, for being able to work with him at least for one year to gain even a slight view from his wisdom

To Dr. Özlem Yalçın, as she never stopped helping me after all the tough times we together went through, for her academic support and for all the experiences she shared with me

To Dr.Pınar Tatar Güner, for her huge support

To Hüseyin Enis Karahan, for his patience to my endless questions, teaching me critical thinking and for his comments to guide me in my future plans

To every single person who did not hesitate to donate their blood for my experiments

To Özge Atcı, Berk İpek, Zeynep Küçüksümer, Alper Turgut and Bahar Atay for their great contribution to my experimental work and their kind companionship in the lab

To Prof. A. Levent Demirel, for sharing his wise scientific knowledge and for leading me improve myself academically

To Dr. Annamaria Miko, for making me become who I am, for her patience, for her infinite support which I know by heart that she will be around whenever I need her, for teaching me never stop believing and hoping in order to achieve my goals and for being an idol to my future academic career

To Ceren Şeref, as she has changed many things in my life, for making life more meaningful and joyful at the same time, for standing behind me whenever I feel close to falling and for solidifying the meaning of a “true friend”

And lastly to my precious family, for assuring me for their support whether I become successful or not, for calming me whenever I tend to be nervous, for smiling with me when I smile, for crying with me when I cry and merely, for being who they are.

I would like to dedicate my thesis to Prof.Oğuz Kerim Başkurt, promising to fulfill his objectives as far as I am able to.

TABLE OF CONTENTS

INTRODUCTION 1

1. Mechanical forces involved in circulatory system 1

1.1. Shear stress 1

1.2. Erythrocytes 8

1.3. Regulatory mechanisms of erythrocyte deformability 12

1.4. Artificial Assist Devices and Blood Trauma 14

1.5. Methods for decreasing the mechanical damage 17

1.6. Mechanical trauma and other blood cells 17

1.7. Aim of the study 18

MATERIAL AND METHODS 19

2.1. Subjects, sampling and erythrocyte suspension preparation 19

2.2. Hemorheologic Parameters 19

2.3. Hematological Parameters 20

2.4. Biochemical parameters 20

2.5. Experimental Protocol 21

2.6. Data analysis 22

2.7. Statistical analysis 22

RESULTS 24

3.1. Hemogram results 24

3.2. Erythrocyte morphology before mechanical stress exposure 24

3.3. Erythrocyte deformability responses to continuous shear stress 25

3.4. Intermittent vs. continuous shear stress application 30

3.5. Free Hb analysis of damage models 34

3.6. Erythrocyte deformability response to oxidative damage 34

3.7. Erythrocyte deformability response to metabolic depletion 38

DISCUSSION 43

BIBLIOGRAPHY 50

LIST OF TABLES

Table 1.1: Shear stress – exposure time relation 16

Table 3.1: Hemogram results of volunteers for each set of experiment 24

LIST OF FIGURES

Figure 1.1: Two types of flow conditions: (a)- Laminar and (b)- Turbulent flow 1
Figure 1.2: Schematic representation of a vessel lumen 3
Figure 1.3: Photomicrograph of human red cells tank-treading in the rheoscope..... 5
Figure 1.4: Parachute-like deformation of red blood cells in the micro-channel capillary flow..... 5
Figure 1.5: Shape change of erythrocytes to pass through the capillaries 9
Figure 1.6: Diffraction pattern from stressed normal human erythrocytes 9
Figure 1.7: Model of reversible deformation of erythrocyte membrane 11
Figure 1.8: Mechanisms of blood damage 14

Figure 3.1: Microscopy images of erythrocytes obtained from subjects before (control) and after treatments..... 24
Figure 3.2: Plasma Free-Hemoglobin measured at 300 s of continuous exposure to shear stresses .. 25
Figure 3.3: Elongation indexes (EI) measured at shear stresses between 0.3 and 50 Pa 27
Figure 3.4: Curve-fit parameters describing the elongation index-shear stress relationship 28
Figure 3.5: Individual donor sensitivity to shear stress (mechanical damage sensitivity) of red blood cells..... 29
Figure 3.6: The time constant of the change in RBC deformation..... 30
Figure 3.7: Elongation indexes for continuous and intermittent..... 31
Figure 3.8: Curve-fit parameters describing the elongation index-shear stress relationship for continuous and intermittent SS 33
Figure 3.9: Free Hb concentrations of oxidative stress and metabolic depletion model..... 34
Figure 3.10: Elongation indexes (EI) after hydrogen peroxide treatment 35
Figure 3.11: Curve-fit parameters describing the elongation index-shear stress relationship after hydrogen peroxide treatment. 37
Figure 3.12: Mechanical damage sensitivity after hydrogen peroxide treatment. 38
Figure 3.13: Elongation indexes (EI) measured at the first and third days of metabolic depletion 38
Figure 3.14: Curve-fit parameters describing the elongation index-shear stress relationship at first and third day of depletion..... 41
Figure 3.15: Mechanical damage sensitivity at first and third days of metabolic depletion. 42

NOMENCLATURE

Ca	:	Calcium
cP	:	Centipoise
eNOS	:	Endothelial Nitric Oxide Synthase
EI	:	Elongation Index
fL	:	Femtoliters
Hb	:	Hemoglobin
Hct	:	Hematocrit
K^+	:	Potassium
KH_2PO_4	:	Potassium phosphate
MCHC	:	Mean Corpuscular Hemoglobin Concentration
MCV	:	Mean Corpuscular Volume
η	:	Viscosity
Na^+	:	Sodium
NO	:	Nitric Oxide
Na^+-K^+-ATPase	:	Sodium-potassium-ATPase
P	:	Pressure
Pa	:	Pascal
PVP	:	Polyvinylpyrrolidone
Q	:	Flow
r	:	Radius
SS	:	Shear stress
V	:	Flow Velocity

INTRODUCTION

1. Mechanical forces involved in circulatory system

Similar to other fluids, blood tends to flow from higher pressure regions to lower pressure regions. Blood flow through circulation is maintained by heart as it generates a balance between high and low pressure. Contraction of the heart by acting as a pump starts the blood motion (85). Arterial tree consists of large muscular and elastic arteries, arterioles and precapillaries. It is subjected to hemodynamic forces formed by heart which varies in magnitude, frequency and its direction widely (86). Such hemodynamic forces acting on the vasculature are classified in two groups: Pressure and shear stress (SS). Pressure is generated by cardiac contraction and acts perpendicular to vessel wall while SS is generated by blood flow and acts parallel to vessel wall (54, 77, 92).

1.1. Shear stress

1.1.1. The Nature of shear stress

SS is defined as the parallel force acting on fluid segments in laminar flow (8). The SS associated with blood flow is the tangential force acting on the endothelial surface of blood vessels (77). Other than SS, cyclic strain is another factor that acts on the vessel walls to induce blood pressure as the walls are stretched with flow (54). Within the vasculature, SS exists due to the friction generated by the blood flow through vessel walls. Pressure, circumferential stretch or strain and SS are considered to be the mechanical forces affecting the vessel walls (77).

Blood cells are exposed to longitudinal shear forces within the vessel (100). Flow behavior shows differences depending on the magnitude of SS while the SS depends on inner vessel diameter, flow rate, viscosity and pulsatility (100). For laminar flow, liquid particles flow parallel to the tube wall by moving in adjacent planes with a regular flow behavior (8). In higher shear regimes the flow behavior changes from laminar to turbulent, which induces swirls and irregular flow manners. The differences in laminar and turbulent flow behaviors are shown in Figure 1:

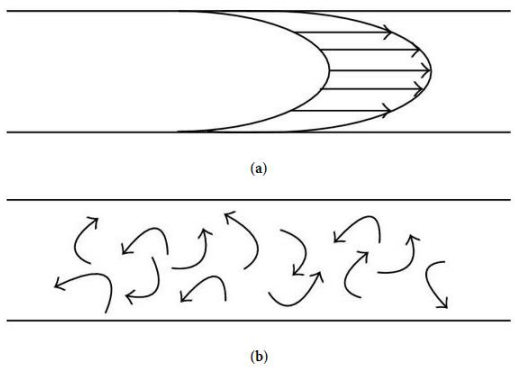

Figure 1.1: Two types of flow conditions: (a)- Laminar and (b)- Turbulent flow (37)

1.1.2. Factors affecting shear stress

SS is defined by Poiseuille's Law (54). It has a magnitude and direction whereas it is defined as a vector mathematically. SS provides the fluid flow within cylindrical tubes and expressed by dyn/cm^2 which is basically the force acting on a unit area (34). By this definition, SS can be related to viscosity (η), flow rate (Q), π constant and vessel radius (r) as follows:

$$\tau = \frac{4\eta Q}{\pi r^3} \quad (1)$$

SS is estimated by shear rate and whole blood viscosity as well as the vessel radius, *in vivo* (84). Pulsatile nature of blood flow causes a variance within the individual cardiac cycles and thus the velocity profile shows inconsistency for its parabolic trend (100). However, this variance can be computed by modeling the flow within both the small and large arteries of a cardiovascular network. Thus velocity profile, flow rate and wall SS can be analyzed more accurately. SS changes depending on the blood behavior mostly due to vessel diameter and distance from the heart (100). It can be seen from Poiseuille's law that with changing diameter, i.e. from arteries to capillaries, SS differs in magnitude. Blood has a non-Newtonian flow manner; the SS to shear rate relation is not linear and viscosity varies with respect to shear rate at a given temperature as well as the vasculature (80). Furthermore, blood is shear-thinning as at high shear rate regimes, a decrease in viscosity is seen (100).

1.1.3. Influence of viscosity on shear stress

Regarding the blood flow, one of the main parameters is viscosity, which is known to be resistance to flow (80). Since blood flow is non-Newtonian, viscosity changes with respect to shear rate but varies with temperature as well. A schematic representation of vessel lumen to express viscosity can be found in Figure 2:

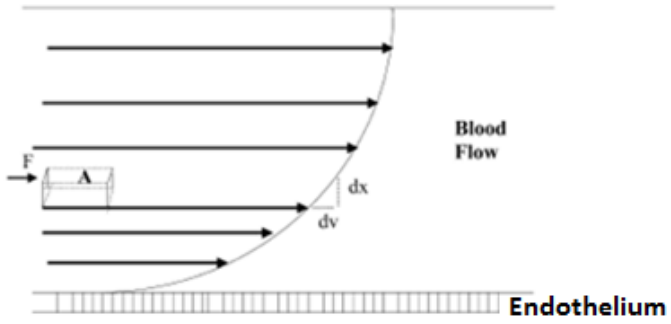

Figure 1.2: Schematic representation of a vessel lumen. The curved line represents the flow velocity profile in laminar flow. The viscosity (unit: Poise) is expressed as a ratio of shear stress to shear rate, where the shear stress (unit: dynes/cm^2) is the force (*F*) parallel to the direction of flow per unit area of fluid sheared (*A*), and the shear rate (unit: second^{-1}) is the velocity gradient between adjacent layers in laminar flow (80)

Although blood is considered as solid-liquid suspension, it can also be thought as a liquid-liquid emulsion due to erythrocytes' liquid-like behavior when exposed to shear (8). With blood being a non-Newtonian fluid and thus having a variety of viscosity values for different shear rates and SS, rotational viscometers are used to measure viscosity over a shear rate range (8). In fact, due to shear thinning behavior of blood, low SS or shear rate values generates a high viscosity while viscosity decreases with increasing SS (8). Plasma, on the other hand, is a Newtonian fluid which means the plasma viscosity is independent of the shear rate.

Hematocrit value plays an important role on blood viscosity (8). Since hematocrit is the ratio of erythrocyte volume to the total blood volume, it provides information about the concentration (100). Elevated hematocrit levels, which indirectly increases the cellular components such as Hb, causes an increase in the blood viscosity (8). Furthermore, by increased hematocrit, laminar flow is disrupted. Blood viscosity is higher than plasma viscosity due to the cellular components and this difference can be expressed by calculating the relative viscosity as the ratio of blood viscosity to plasma viscosity (8). Another determinant of viscosity is cytoplasmic viscosity which is determined by intracellular Hb (16) content (67). After reaching the threshold Hb concentration, which is 37 g/dL, cytoplasmic viscosity increases exponentially (67).

Lipowsky et.al investigated the changes in blood viscosity by altering the hematocrit values at constant shear rate and vice versa (56). Results showed that for low hematocrit values, viscosity is not significantly affected by shear rate. On the contrary, as hematocrit level is gradually increased the effect of shear rate on viscosity increased. At arteries that have ~300 sec^{-1} shear rate, for instance, the viscosity is recorded as 3.5 cP for a standard hematocrit value of 45%, while at lower shear rate regimes such as sites having ~5 sec^{-1}, viscosity increased to 10 cP.

Since vessel diameter is crucial for the flow dynamics, it is important to understand the basic principles of microcapillary flow as well as the behavior within arteries (85). For this purpose*, in vitro*

studies are designed aiming to mimic the microcapillary flow behavior (105). Physiologically, diameters of erythrocytes are larger than that of some capillaries. Thus, in such flow conditions erythrocytes change their shape from biconcave discs to a parachute-like shape by reorganizing their cytoplasm to pass through microcapillaries. To mimic the microcapillary flow behavior of erythrocytes, couette-type viscometers are usually used to expose erythrocytes to defined amount of SS for a given time (39). Other than couette type viscometers, cone-plate type systems might be used as well to mimic the circulation and flow behavior of blood.

1.1.4. Influence of flow rate on shear stress

Under low shear conditions, the viscosity tends to increase as erythrocytes form clusters to aggregate. On the other hand, high shear conditions cause decreased viscosity as aggregates are separated by the applied shear. Aggregation under low shear flow is due to the biconcave disc shape of the erythrocytes, while the decreased viscosity under high shear flow is caused by deformed erythrocytes (30). Normal shear flow generates two motions for erythrocytes within the vasculature: Tank-treading and tumbling (28). When erythrocytes are exposed to shear, in addition to elongation, their membrane moves around itself (31). This motion is known as tank-treading motion. The tumbling motion, which is much more like a wheel-like motion is seen under low shear conditions, and this motion can change into tank-treading motion for higher shear stresses (28). In other words, erythrocytes behave like a solid body under low shear (30).

Tank-treading motion occurs due to the rotation of the membrane around its cytoplasmic fluid under a shear flow (107). External SS is transferred across the cell membrane to the cytoplasm in order to induce internal circulation (112). By this flow behavior, apparent blood viscosity decreases. A photomicrograph of tank treading motion was obtained via a counter rotating cone-plate shear chamber (see Figure 3) below:

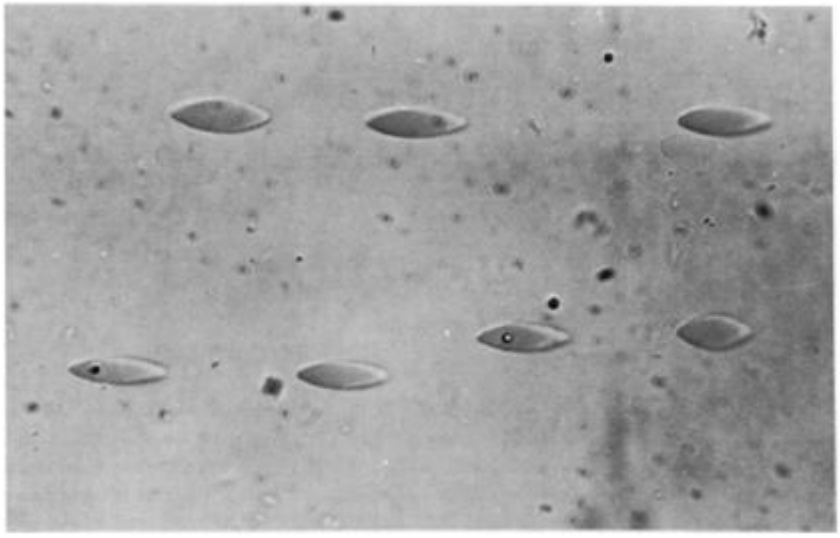

Figure 1.3: Photomicrograph of human red cells tank-treading in the rheoscope. Cells suspended in buffered saline with dextran added; viscosity = 30 cP. Applied shear rate = 200 s-'. Polystyrene beads are attached to membranes of two of the cells (107)

There are many approaches to observe the blood flow *in vivo* such as fluorescence labeling, optical imaging and photoaccoustic and photothermal cytometry. Fit-C dyes were used to label erythrocytes flowing in the blood (65). To investigate blood flow behavior *in vitro*; vasculature flow was mimicked by capillary flow and the parachute-like shape that erythrocytes took under flow is observed (Figure 4):

Figure 1.4: Parachute-like deformation of red blood cells in the micro-channel capillary flow and the deformability defined by the lengthwise to crosswise ratio of erythrocyte deformation (65)

Depending on the vessel geometry and radius, erythrocytes undergo either symmetrical or nonsymmetrical shape change, being parachute and slipper-like respectively (112).

Bishop *et al.* examined velocity profiles in venous microvessels which have 45 to 75 µm diameter. Velocities were in between 0.3 and 14 mm/sec and pseudo shear rates were 3-120sec^{-1} (15). Blunted erythrocyte velocity profile was recorded under low shear conditions. It is stated that flow within the microcirculation determines the peripheral resistance. Considering the Newtonian relationship, flow

is proportional to the fourth power of vessel diameter. This clearly indicates the greater role of diameter on SS (97).

1.1.5. Influence of vessel structure and geometry on shear stress

Blood flow rate and velocity profiles show differences regarding the arteries and veins as they are exposed to different SS (77). Physiological range for arterial SS is between 10 to 70 dynes/cm^2 whereas veins have a lower range between 1 to 6 dynes/cm^2. Local geometry of blood vessels alters the magnitude and directionality of SS (24). Arteries and veins show differences in terms of viscosity (96). The magnitude change of blood viscosity might be on the order of 10^1 to 10^2. By the principles of Poiseuille Law, arterial SS was estimated to be 1.5 Pa (84). Arteries and arterioles both show a flattened and parabolic trend regarding the velocity profiles. Arterial velocity profile does not generate a full parabola due to unsteadiness and short entrance lengths while that of arterioles do not develop a full parabola either, since viscous forces dominate the center of these vessels and branching occurs. Due to having flattened profiles, shear rate (also known as velocity gradient relative to the vessel radius) is higher close to the arterial wall whereas it is lower at the center. On the contrary, viscosity is higher at the center which is known to be due to axial migration (84). Blood viscosity is at its minimum within the arteries while it reaches maximum at venous circulation (96).

In vivo and *in vitro* analyses vary with respect to rheological properties. Compared to the cylindrical tubes used in *in vitro* experiments, vessel geometry, especially for microvasculature, is highly complex and has extreme branching (8). Varying of the diameters and length causes irregularity within the vessel and flow manner. Therefore, estimations made by in vitro observations using straight glass tubes might not match that accurately with the *in vivo* observations (76). Furthermore, orientation versus gravity of individual microvessels shows differences and formation of a cell free layer is mostly orientation-based. As blood vessels are elastic, vascular geometry and flow resistance can be modified to increase their diameter as a response to pressure increase. To estimate the arterial wall SS, high peripheral resistance should be taken into account (84). To compare *in vivo* and *in vitro* studies, increased flow resistance *in vivo* due to irregularity in geometry should also be taken into account (76).

1.1.6. Shear stress in circulation

Blood flow in circulation is quite different from flow in a straight tube. There are two important reasons for this difference: 1- the pulsatile nature of blood flow and 2- variations within the vessel geometry within the whole circulation (29). These factors cause variations in the blood flow manner throughout the circulatory system, which are mostly seen at points of vessel curvatures. Blood flow

at such points is low since the wall shear rate is various throughout the cross sectional area of the vessel; on the contrary, other side of the vessel wall has a higher blood flow rate (92). In addition to the vessel curvatures, vessel bifurcations cause variation of flow rate within the circulation. At bifurcation points, flow rate is maximum at the inner wall, which includes the bifurcation and minimum at the outer wall (83).

Irregularity of vessel geometry has been identified as a reason of variation between *in vitro* and *in vivo* flow behavior (76). In other words, extreme branching generates a complexity in *in vivo* flow (8). Complexity of *in vivo* blood flow comes from bifurcations occurring within vessels, curvatures and the pulsatile nature (92).

The blood flow dynamics in circulation depends strongly on the microvascular networks composed with short irregular vessel segments which are linked by numerous bifurcations. Curving of a vessel generates a greater velocity for blood flow through the outside wall of the vessel rather than the inside wall (92). On the contrary, bifurcation of a vessel causes a slower blood flow through the outer wall while the blood flow is the fastest near the flow divider. Diameter changes occur at the branching points of vessels (44). Vessel segments between bifurcation points express a cylindrical structure. Average wall SS increases from larger to smaller arteries at each bifurcation (100). Curvatures and bifurcations disrupt the steady laminar flow and develop regions of separate flow including the recirculation sites (86). These secondary flows dominate the SS within the regions.

In addition to alterations of blood flow manner caused by bifurcations and curvatures, pulsatile alterations regarding the velocity and direction of the blood flow varies the wall SS (92). In fact, wall SS changes due to cardiac cycle which has an oscillatory pattern.

High magnitudes of SS induce vessel wall thickening which might trigger atherosclerosis (77). In addition to being multifactorial, focal distributed plaques in curvature or bifurcation segments and branching points of vessels indicate the major role of vessel geometry and fluid dynamics on localization of the plaque formation (92). Magnitude and directionality of SS are altered when the local geometry changes due to presence of a plaque (24). Highest risk for atherosclerosis is associated either with segments with low wall SS or those with highly oscillatory wall SS (92).

Blood flow is also affected by the nature of cardiac cycle (systole and diastole). Blood velocity is high during systole while it is relatively low in diastole (84). Since diastole constitutes two thirds of the cardiac cycle, its effect compared to systole is greater for mean wall SS calculation. During systole, increase in the wall SS and pulse pressure is limited.

To estimate all the parameters given, SS should be calculated appropriately regarding the complexity of vessel geometry and flow behavior. Correct measurement of SS requires an experimental approach. One example for such an experimental approach can be given as MR velocity mapping (92). SS is measured by mean flow rates and arterial inner diameters (100). Calculating the

wall SS requires an estimation of the slope of a velocity profile including two or three velocity values obtained near the vessel wall (92).

1.2. Erythrocytes

1.2.1. Membrane Lipids

Erythrocyte membrane is the main determinant of shape change and is composed of a lipid bilayer which is involved in regulation (67). The lipid bilayer is arranged asymmetrically and therefore, 75% to 80% of the phospholipids are distributed in the outer monolayer whereas the inner monolayer retains most of the aminophospholipids (38). This arranged state is maintained by two orientation enforcing mechanisms, known as the passive and active enforcement. Passive phospholipid stabilization is obtained by interaction of phosphatidylserine molecules with band 4.1 and spectrin (38). Active enforcement of orientation is based on ATP-dependent phospholipid translocating activity.

1.2.2. Membrane Proteins

Erythrocyte membrane plays a pivotal role entangled with its structure, geometry and function (26). Erythrocyte membrane is composed of a lipid bilayer and contains external and integral proteins (59). Reorganization of the membrane is provided by lipids and the proteins (67). Integral proteins extend through the bilayer while external proteins do not penetrate inside (17). External proteins provide membrane stability to erythrocytes and this causes erythrocytes to maintain their shape. There are three main proteins serving for regulation of the membrane network and are given as follows: spectrin, actin, protein 4.1 and protein 4.9 (actin-capping protein). Skeletal proteins provide rigid support and stability to erythrocytes and are involved in shape change (67). Membrane stability depends on spectrin-actin-protein 4.1 interaction (21).

1.2.3. Erythrocyte deformability

Erythrocyte deformability, defined as the ability to change shape under shear stress, is known to be one of the main determinants of the blood flow, especially in microcirculation (5). When erythrocytes are exposed to SS, they elongate and thus undergo a shape change. Erythrocytes have an excess surface area compared to their volume being 142 μm^2 and 90 fL, respectively (70). The surface to volume ratio does create a 40% of excess surface area and this excess surface area provides an easier passage through capillaries smaller than erythrocytes within circulation without fragmentation (Figure 5) (8). Moreover, since erythrocytes lose their nucleus during maturation, their

shape changing ability strengthens (96). Erythrocyte deformability significantly affects regional flow conditions; in case of a decrease in deformability the flow is altered (95).

Figure 1.5: Shape change of erythrocytes to pass through the capillaries (8)

There are several methods to measure deformability such as micropore filtration, micropipette aspiration and diffraction pattern analysis (5). For instance, filtration methods are used by applying different pressures and measuring the rate at which erythrocytes traverse from pores with having defined sizes (67). On the other hand, diffraction pattern analysis can be made by using ektacytometry. An ektacytometer comprises two optically clear concentric cylinders with a ~0.5 mm gap in between (40). Diffraction pattern and elongation of erythrocytes is analyzed in response to shear as the method is based on couette viscometer principles and erythrocytes are exposed to shear by rotation of the outer cylinder. An example for diffraction pattern analysis is shown in Figure 6:

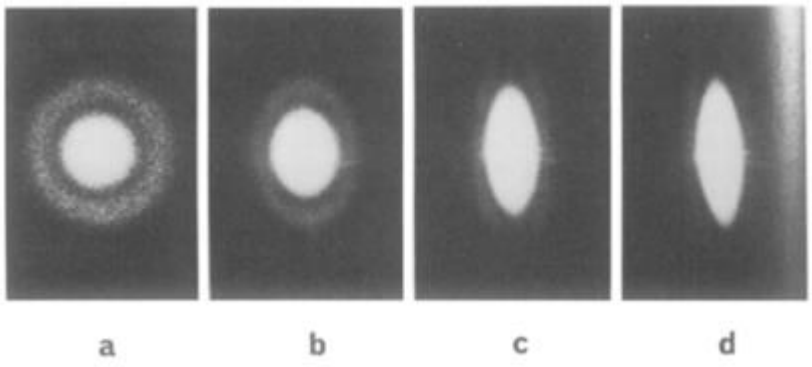

Figure 1.6: Diffraction pattern from stressed normal human erythrocytes. (a) No stress, (b) 12.5 Dyn/cm^2, (c) 50 Dyn/cm^2, (d) 125 Dyn/cm^2 (40)

From the diffraction pattern analysis, the most important parameter obtained is elongation index (EI) (40). It is calculated by the formula (A-B)/(A+B) where A is the long axis of the pattern and B is the short axis.

Cellular deformability is expressed in terms of cytoplasmic viscosity, cellular geometry and membrane material properties (67). Both skeletal and integral proteins are involved in the shape change. Shape change is induced by the continuous movement of erythrocyte membrane around cytoplasm while chemical perturbations induce the alteration. In addition to deformability, membrane stability, which is the maximum extent of deformation of membrane that can undergo until it cannot deform reversibly (21) is also important; erythrocyte deformability and stability are regulated by the interactions of different proteins.

Cytoplasmic viscosity is mainly determined by the Hb concentration which should be in a range between 27-37 g/dL and corresponds to viscosity values of 5-15 centipoises (70). Within given range, effect of the cytoplasmic viscosity on erythrocyte deformability is negligible and the viscous distribution of forces acting on the cell membrane is the main determinant of erythrocyte deformability (68, 71, 115). For higher concentrations of Hb; however, cytoplasmic viscosity increases exponentially with Hb concentration. Hb concentrations of 40,45 and 50 g/dL generate a viscosity of 45, 170 and 650 cP, respectively (70). In case of water efflux from the erythrocyte, cellular dehydration takes place. Increase in mean corpuscular Hb concentration (MCHC) and crosslink between Hb and membrane proteins may take place to limit the movement of spectrin molecules which leads to disrupt the erythrocyte deformability.

Conformation of spectrin regulates the erythrocyte deformability. In its nondeformed state, spectrin molecule adopt a folded conformation whereas during the deformation skeletal network is rearranged (21). Certain spectrin molecules are uncoiled and others become more compressed and stay folded. Reversible deformation causes alterations in the geometric shape but surface area remains constant while SS causes spectrin molecules to extend linearly (Figure 7):

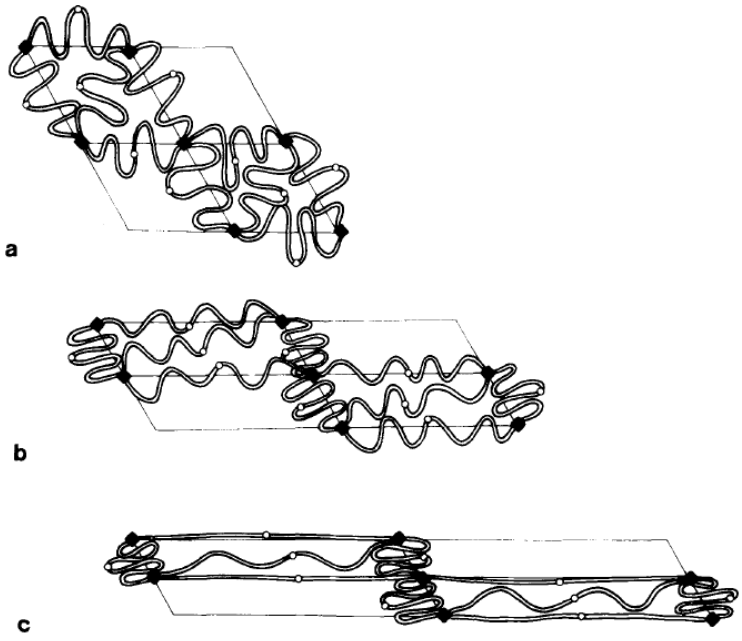

Figure 1.7: Model of reversible deformation of erythrocyte membrane. Reversible deformation occurs with a change in geometric shape but a constant surface area. a: Non-deformed membrane. With increased shear stress, the membrane becomes increasingly extended (b and c). Further extension of the membrane beyond that shown in c would result in an increase in surface area and the breaking of junction points (21)

Pfafferot *et al* examined the decrease in deformability by incubating blood with malonyldialdehyde, a crosslinking agent (79). Counter rotating cone-plate viscometer was used at low shear conditions applying 2.5 to 25 dynes/cm^2 SS. Decreased deformability and increased membrane rigidity was recorded, which attributed the deformability changes to lipid peroxidation and polymerization of membrane constituents. Another study investigated the crosslinking between spectrin and Hb molecules induced by hydrogen peroxide (98). Methemoglobin formation is seen upon the treatment. It was concluded that spectrin may regulate the cell shape and surface characteristics by attaching to the lipid bilayer and integral membrane protein, band 3. Role of the spectrin is pivotal for regulation of deformability and stability (98). Examples summarize that membrane interactions are crucial for erythrocyte deformability.

Glutaraldehyde is another fixative used in crosslinking (9). The impairing effect of glutaraldehyde is recorded as the deformability changes. Concentration range was chosen as 0.005-0.020% to see the gradual change in deformability. Alternatively, heat treatment is used to observe impairment in deformability (9). Heating erythrocyte suspensions at 48^{o}C for 5 minutes generates a permanent damage due to crosslinking between cytoskeletal proteins since heating causes proteins to undergo denaturation and their structure is disrupted (118).

Another important parameter influencing the erythrocyte deformability is osmolarity. The osmotic pressure of a suspending medium should be in a definite range because otherwise an

increase in osmolarity causes a decrease in the cell volume though surface area remains constant and thus deformability is altered (67, 68, 71). Increased osmolarity may trigger the interaction between Hb molecules.

During deformation, erythrocytes release ATP in response to SS (112). ATP release increases with increased SS magnitude. ATP is crucial for erythrocytes because lack of ATP causes membrane loss, fragmentation and echinocyte formation (23, 94, 114).Echinocyte is one of the impaired erythrocyte structures which is formed as a sphere covered by spikes (41). Lack of ATP occurs as blood is stored since it becomes metabolically depleted. Oxidative mechanisms are involved in the process and reduced deformability is obtained (14).

1.3. Regulatory mechanisms of erythrocyte deformability

1.3.1. Effect of nitric oxide on erythrocyte deformability

Endothelial cells play an important role in the regulation of vasculature as they are aligned with wall SS (85). These cells are mechanosensitive and sense the shear with specified receptors. Left ventricular ejection generates a force on artery wall which is sensed by the endothelial cells (84). Wall SS causes alignment of endothelial cells and this depends on the magnitude of the stress. Higher SS conditions generate more elongated cells. Sensing the wall shear stress is vital for the regulation of vasculature for appropriate tissue perfusion and vasomotor motions which is known as smooth muscle tonus.

Modulation of endothelial function is generated by wall shear stress which is defined by the fluid velocity and local viscosity (117). Axial migration is one of the key factors for the endothelial function as it causes a cell free layer near the vessel wall while the flow reaches it maximum level at the center. Aggregation is important in this regard since it will mediate the axial migration. The effect of aggregation was tested by enhancing the aggregation with a co-polymer coating to alter surface properties of erythrocyte and significant differences in vascular hemodynamics were recorded related mostly to flow resistance (4).

Mechanotransduction, signaling mechanism within the cells, is initialized by the pressure-sensing ability of the endothelial cells. Nitric oxide (NO) plays the key role for vasomotor regulation. Cellular level homeostasis is provided by feedback regulation of intracellular mechanics and signaling in response to stress (22). Endothelial nitric oxide synthase (eNOS) is the enzyme to synthesize nitric oxide from endothelial cells within the blood vessels. Endothelial cells sense the pressure changes within the vessels using their receptors (86). In addition to its role on the vasomotion, NO plays a vital role on erythrocyte deformability and is tested upon usage of NO donors / inhibition of eNOS

(12). It is stated that potassium influx through cell membrane might be involved in regulation of erythrocyte deformability by NO. By this purpose, function of potassium channel was tested as well and the results reveal that if potassium leakage from erythrocyte is prevented, by using the channel blocker in this case, NO effect is mediated.

It is known that NO is a crucial regulatory molecule regarding erythrocyte deformability (13, 18, 19, 47). Baskurt *et al.* demonstrated the regulatory role of NO on erythrocyte mechanical properties (12). According to their findings, a definite concentration of NO is essential to maintain erythrocyte deformability. If the NO concentration exceeds that concentration, however, erythrocyte deformability is adversely affected. Despite the uncertainty of intracellular signaling cascades NO uses for the regulation, evidences exist that NO regulation of erythrocyte deformability takes place by K^+ channels. Basically, NO prevents the K^+ efflux from the erythrocyte membrane and regulates erythrocyte deformability (12). Regulatory role of NO on deformability was to be examined upon exposure to shear stresses which is known to damage the erythrocytes. Studies proved that NO had an improving effect on erythrocyte deformability when damaging shear stresses were applied (12). Inhibition of NO during shear stress exposure did not result in an additional impairment. These show that NOS inhibitors decreasing the NO amount in erythrocyte cytoplasm and mechanical damage are parallel in functioning (K^+ efflux from erythrocyte membrane). Usage of K^+ channel blockers is protective against the mechanical damage of erythrocytes following shear stress exposure (12).

1.3.2. Effect of calcium on erythrocyte deformability

Cytoplasmic viscosity which plays a vital role on rheology regarding the flow resistance is stabilized by cation and water regulation (45). The energy supplied by erythrocyte metabolism is mostly used by active ion pumps. The main ones are Na-K-ATPase and Ca-ATPase and are involved in generating a balance for the maintenance of low Na, high K and low Ca concentration. The total calcium content for normal erythrocyte is 5 µmol/L (38). Regarding this reference concentration value, increased intracellular calcium concentration impairs the deformability (67).

Increase in the intracellular calcium concentration is known as “Gardos Effect” (45). With the mentioned increase, Ca dependent potassium ion channels are opened and K flux from intracellular to extracellular medium is seen along with water loss. Gardos effect causes disruption in the regular shape changing ability of erythrocytes, known as deformability. Crosslink between membrane proteins and echinocyte formation are the results of Gardos effect (45).

1.4. Artificial Assist Devices and Blood Trauma

Ventricular assist devices (VAD), dialysis machines, heart valves and cardiopulmonary supports are among some artificial devices. Assist devices and artificial organs are widely used either to extend or to save the lives of patients who await organ transplant. Blood damage caused by artificial devices determines how efficient and safe they are. Main reason for blood damage is exposure to non-physiological conditions such as nonphysiological SS, turbulent flow, cavitation (88).

The main damage mechanism includes over-stretching or fragmentation of an erythrocyte subpopulation which induces the release of free Hb into plasma (78, 116). This phenomenon is blood damage, also known as hemolysis. Two other mechanisms leading to blood damage are the activation or dysfunction of platelets-leukocytes and sub-lethal erythrocyte trauma. As well as the activation of platelets and leukocytes, increase in inflammatory mediators is also involved. Sub-lethal trauma generates an increase in erythrocyte aggregation and a decrease in erythrocyte deformability. Listed mechanisms can end up with problems such as anemia, endothelial dysfunction, hypoxia due to poor capillary perfusion, thrombosis and infection (Figure 8).

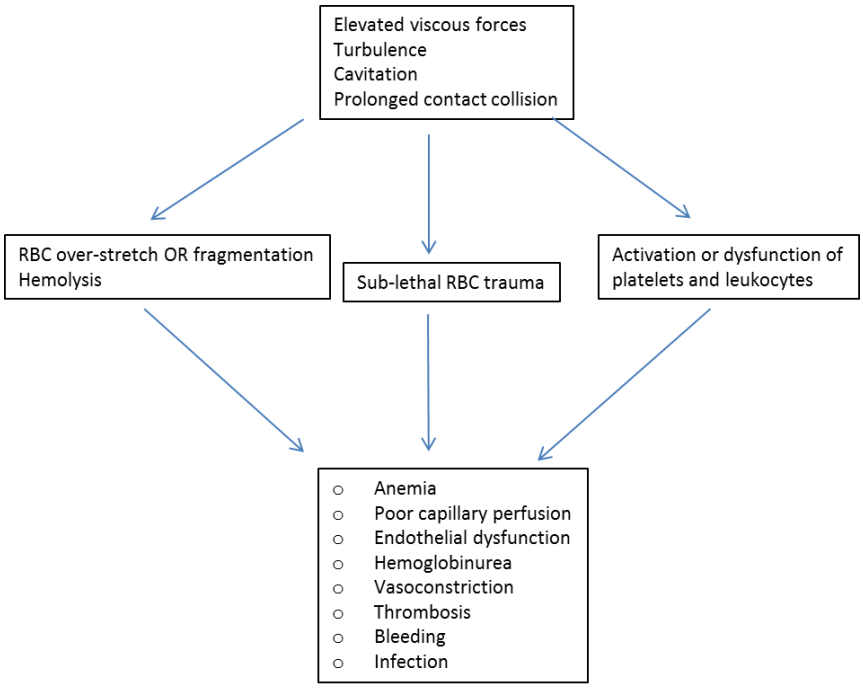

Figure 1.8: Mechanisms of blood damage (110)

1.4.1. Assist devices and artificial organs

One of the most commonly used artificial devices is ventricular assist devices (VAD). Heart assist devices might be considered as a transition step to organ donation. There are three time periods for the use of the artificial devices: short term use (0-4 weeks), medium use (1-6 months) and long term use (>6 months) (53).

Blood cells are exposed to non-physiological conditions while contacting with the artificial devices. Due to the collisions between blood cells and the non-biological surface of the artificial devices, blood damage occurs which mainly affects erythrocytes (103). Regarding the time periods for the use of artificial devices, erythrocytes are traumatized and then damaged irreversibly (53). Chronic anemia, for instance, is seen in patients using artificial devices. Moreover, anemia might be due to decreased erythrocyte life span associated with the sub-lethal blood trauma (91). Magnitude of the damage depends highly on the exposure time and SS. Blood damage may trigger functional impairment of cells and thrombotic events.

1.4.2. Mechanical Blood Trauma

Physiological SS is known to be in between 1-10 Pa (81). Almost a ten-fold increase in this SS value is seen in the presence of artificial devices (27). The non-physiological conditions generated by artificial devices cause denaturation of proteins (103). Decreased deformability and increased aggregation of erythrocytes occur as a result of mechanical alterations.

Hemolysis and thrombosis are two main artifacts of artificial devices (3). Hemolysis occurs when erythrocyte membrane is damaged and free Hb diffuses out of the cell. Free Hb might alter the vessel radius by influencing the nitric oxide (57). Activation of platelets and leukocytes trigger the thrombotic events as well as the alteration in the NO function (6). Platelets are the first to diffuse to interaction site between the artificial device and blood. In addition to activation of platelets, bleeding and infection may be seen. Due to these factors, estimation of hemolysis is clearly required to optimize artificial devices (32). Approximately 300 Pascal is assumed as the hemolytic threshold (73).

Erythrocyte aggregation causes a plasma rich layer close to the endothelium and this reduces the vasodilator release due to reduced wall shear loading. Increased aggregation is known to induce inflammatory responses as well (1). In addition, concentration of plasma fibrinogen, immunoglobulin and other macromolecules do increase.

Optimization of artificial devices is vital to increase the compatibility when used within the body and this is possible only with detecting the hemolysis ratio. Hemolysis ratio can be defined as the ratio of free plasma Hb concentration to the whole blood Hb concentration (32). Normalized hemolysis index is obtained by standardization of the given ratio with respect to hematocrit value, flow rate within the device and exposure time (72).

1.4.3. Sub-hemolytic Blood Trauma

Erythrocytes can be damaged below the hemolytic threshold SS as well. This phenomenon is defined as sub-hemolytic damage that usually brings decrease in deformability and increase in

tendency for aggregation as well as the morphological changes (60). These alterations significantly affect the tissue perfusion which is related to the flow mechanics of erythrocytes. Sub-hemolytic trauma also alters the cell stability as well which decreases the hemolytic threshold (33). It is important to record impairment of erythrocyte function and structure far before the hemolysis to obtain more relevant test methods of hemolysis (46).

The amount of sub-lethal blood damage compared to total lysis is hard to detect and there are two important parameters regarding the sub-lethal damage: Magnitude of the SS and exposure time to the applied shear. Anemia is seen in patients using artificial devices because artificial devices generate continuous and mostly non-physiological SS on blood cells (6). SS – exposure time relation is summarized in Table 1:

SS, N/m^2	**Exposure time, sec**	**Source**
4000	0,00001	Blackshear, 1972
300	0,4	Paul et al., 2003
200	0,6	Paul et al., 2003
120	15	Baskurt et al., 2004
56	180	Lee et al., 2004
10	144	**Physiological ss**

Table 1.1: Shear stress – exposure time relation (6)

Another critical parameter to detect sub-lethal damage is mechanical fragility (43). Mechanical fragility tests comprise exposure to constant mechanical stress by shaking the samples together with sphere beads and thereby generating mechanical damage. There are some artifacts, however, regarding the fragility test. Erythrocyte mechanical properties might show alterations depending on the suspending medium (35). Also storage time and collecting conditions during the tests might affect the mechanical properties as these parameters interfere with increased mechanical fragility.

In order to optimize the artificial devices and define a measurable mechanical damage in blood, it is important to standardize the sub-hemolytic blood damage. In addition the hemolysis ratio, erythrocyte deformability and aggregation, mechanical fragility is used to clarify the blood damage (12). However, these parameters alone might not be efficient to express the amount of blood damage. It should be noted that since the blood damage is mainly associated with the hemolysis, mechanical alterations occurring before the hemolysis therefore might be left underestimated. Since alteration in the blood function and thrombotic events should be minimized to optimize the artificial devices, such standardized parameters are required (11).

1.5. Methods for decreasing the mechanical damage

One approach to minimize the mechanical damage is related to the design of artificial devices. Regarding the device design, flow-induced stress might be calculated using simplified models both for turbulent and laminar flow regions (82). Flow should be continuous within the artificial devices. Computation methods and imaging techniques are widely used to estimate the flow behavior within artificial devices to minimize the artifacts (109). One disadvantage is that for all these estimations using computational methods, only hemolysis ratio is taken into account as the blood damage determining parameter. Sub-hemolytic trauma, therefore, appears to be pivotal for more relevant estimations (53).

Maintenance of appropriate plasma albumin level is important to diminish the blood trauma caused by artificial devices (42). Damage caused by mechanical agitation was to be eliminated by a polymer, poloxamer 188 (2). This polymer also inhibited the platelet aggregation; therefore it was found advantageous in eliminating the thrombic events. Besides these findings, studies show that plasma proteins at certain concentrations have a protective effect regarding the blood damage (102). Another treatment includes urea which improves the effect on erythrocyte deformability as well as decreasing the amount of plasma free Hb (87). Improvement in erythrocyte deformability may also be provided by use of L-carnitine which was confirmed by experimental studies (106). L-carnitine is used as supplementary in case of atherosclerosis or acute myocardial infarction and was recorded to improve deformability in thalassemic patients.

1.6. Mechanical trauma and other blood cells

Other blood cells contacting the artificial organs and ventricular assist devices are also affected from altered flow conditions and interaction with the non-biological surfaces. It is known that leucocytes are damaged while travelling through extracorporeal circulation and decreased in number as well as impaired function (49, 50). Leucocytes are activated by contact with non-biological surface and responsible for the mentioned damage (25, 64, 90). McBride *et al.* stated that after the cardiopulmonary bypass surgery, proinflammatory cytokines (tumor necrosis factor (TNF-α), interleukine-8) are activated in 5 minutes and the activation remains for 2 hours. Then, anti-inflammatory cytokines (IL-10 and IL-1 receptor antagonist and soluble TNF receptor) are produced after 2-24 hours following the cardiopulmonary bypass (61). Reactive oxidative species are generated due to leucocyte contact with the non-biological surface (52, 89, 93).

Thrombocytes are more sensitive to mechanical damage compared to erythrocytes. Brown *et al.* showed that thrombocytes are disintegrated at one tenth of the shear stress damaging the erythrocytes (20). If thrombocyte damage continues, number of thrombocytes is expected to

decrease (111). Thrombocytes are activated in response to shear stress (20, 55). Within this process, role of both the direct effect of shear stress on thrombocytes and adenosine diphosphate (ADP) released by hemolytic erythrocytes causing thrombocyte activation is seen (62). It should be emphasized that thrombocyte activation might trigger the thrombotic risk for patients using artificial organs or ventricular assist devices.

Mechanical blood trauma influences the leucocytes and thrombocytes as well but detection of this mechanical damage is usually obtained by analyzing erythrocytes. Thus, other blood cells were not used in this study.

1.7. Aim of the study

The recent findings generate questions regarding the specific threshold that demarcates a shift from improvement to impairment of RBC mechanics following exposure to SS. Some answers may include: (a) Deformability changes might be investigated as a function of exposure of RBC over a broad range of SS; (b) The effects of applying continuous or intermittent SS should be considered to determine if the time-stress product is of importance; (c) Donor-to-donor variations need to be evaluated by using blood from various subjects to determine whether this so-called subhemolytic threshold may reflect individual sensitivity to high mechanical shears. Another object of the study: the sensitivity, specificity for particular damage model and reproducibility of sub-hemolytic threshold was investigated in normal and damaged erythrocyte suspensions such as metabolic depleted and hydrogen peroxide treated. The present study was designed to address these issues.

MATERIAL AND METHODS

2.1. Subjects, sampling and erythrocyte suspension preparation

All blood samples were collected from male and female healthy volunteers aged between 20-57 years. Vacuum tubes containing heparin as anticoagulant were used to take the blood (15 IU/ml). Sampling of the blood was carried out via placing a tourniquet on the upper arm of the donor. Blood was collected from a prominent antecubital vein. Sampling was concluded within 90 seconds. All experiments were completed within 4 hours following the sampling. Oral consent of each donor was taken before the sampling. The use of human blood was in accordance with The Code of Ethics of the World Medical Association (Declaration of Helsinki). All experimental procedures were approved by the Institutional Review Board, Koc University. Erythrocytes were resuspended in isotonic phosphate buffer saline (Na_2HPO_4: 0.01M, KH_2PO4: 0.0018M, NaCl: 0.137 M and KCl: 0.0027 M; pH:7.4) unless whole blood samples were used.

2.2. Hemorheologic Parameters

2.2.1. Measurement of erythrocyte deformability

Laser diffraction ektacytometry (MaxSis, Mechatronics, Hoom, Netherlands) was used to measure erythrocyte deformability which consists of a co-axial couette type cylindrical shearing system. The inner cylinder contains a laser projecting through the gap between two cylinders and the scattered laser light by erythrocytes is digitally collected and analyzed via software (74). By this technique, flow stress is generated to an erythrocyte suspension prepared in a high viscosity medium. Information about cell deformability is obtained by the diffraction pattern resulting from the laser beam which is transversed by the suspension.

Deformability measurements were recorded by applying shear stress from 0.30 to 50 Pa. corresponding elongation indices to each shear stress were calculated upon the diffraction pattern obtained which is gathered digitally after it is sent from the inner cylinder. Measurements were recorded after diluting the blood suspensions in 6% high molecular weight polyvinylpyrrolidone solutions (Mechatronics, Hoorn, Netherlands) with a dilution ratio of 1/200. PVP has a molecular weight of 360 kDa while the viscosity is 28.9 ± 0.5 mPa.s. Approximately 1 ml of blood suspension in PVP is put through the gap between the inner and outer cylinder. The outer cylinder rotates at a calculated shear rate throughout the measurements to form shear stress. Magnitude of the shear is calculated both by the shear rate and viscosity of the suspending medium. Erythrocyte orientation in response to shear is obtained by the diffraction pattern analysis. Erythrocytes change their shape from sphere to ellipsoidal form proportional to the shear magnitude applied. Diffraction pattern

provides information of elongation index calculated by the formula of (A-B)/(A+B), A being the long axis while B being the short axis of the erythrocyte. All measurements were obtained at 37^{o}C.

Following the deformability measurements, erythrocyte suspensions were exposed to various shear stresses of a broad range (5-100 Pa). Cell stability test was used for the shear exposure and measurements were recorded for 300 seconds. Time dependency was checked as well in the analysis of cell fragmentation and free Hb. Cell stability test was recorded for 120, 150, 200, 250 and 300 seconds for this purpose.

Regression analysis of the data was obtained by Lineweaver Burk equation. The non-linear regression analysis calculates half maximal elongation index and corresponding maximum elongation index. Formula of the Lineweaver Burk equation is as follows:

$$Y = \frac{1}{(SS_{1/2} / EI_{\max})} * \frac{1}{x} + \frac{1}{EI_{\max}} \quad (2)$$

where Y is elongation index, x is the shear stress between 0.30 and 50 Pa. By given equation, one can obtain information about the rate of erythrocyte response to a given shear stress and elongate respectively.

2.3. Hematological Parameters

2.3.1. Analysis of Complete Blood Count

Red blood cell count (RBC), hemoglobin (HB), hematocrit (HCT), mean corpuscular volume (MCV) and mean corpuscular hemoglobin concentration (MCHC) were determined in each blood sample via an electronic hematologic cell analyzer (Micros, ABX Co., France).

2.3.3. Investigation of erythrocyte morphology

Blood samples, following a 1/10 dilution in autologous plasma, were analyzed morphologically via Axio Scope A1 (Zeiss, Munich, Germany) light microscope.

2.4. Biochemical parameters

2.4.1. Determination of plasma free hemoglobin concentration

Free hemoglobin in PVP suspending medium was determined prior to or after the shear stress application via a modified cyanomethemoglobin technique (51). Erythrocyte concentration in PVP was doubled for this measurement compared to the usual LORRCA measurements (See section 2). Each blood sample was collected in a separate Eppendorf following the shear exposure to be centrifuged at 3000 rpm for 5 minutes. 200 µl of supernatant solution of each sample was added to 800 µl of Drabkin (1.1.3 mM potassium dihydrogen phosphate, 0.6 mM potassium ferricyanide, 0.8

mM potassium cyanide in 500 ml 30% Triton-X solution and 1100 ml distilled water) solution. Addition of supernatant to the Drabkin solutions were followed by a 15 minutes of incubation at dark and at room temperature. Absorbance values were recorded at 546 nm after the incubation using spectrophotometry.

2.5. Experimental Protocol

For healthy and modified erythrocytes, such an experimental protocol was followed: 1) Deformability of control (unsheared samples) was measured prior to either continuous or intermittent shear stress. Measurement gave an EI-SS relation for pre-selected SS levels (0.30, 0.53, 0.94, 1.65, 2.91, 5.51, 9.09, 16.04, 28.32 and 50.00 Pa). 2) Suspension previously exposed to shear stress was aspirated from the gap and cleaned with isotonic PBS and new sample was placed in between each shear stress within the cell stability test. With the cell stability test, constant or intermittent shear stress was applied to the blood samples for 300 seconds. 3) Immediately after the cell stability test, deformability measurements were recorded for each corresponding stability test. For erythrocyte models (unhealthy cells), only continuous shear stress was applied.

2.5.1. Application of continuous and intermittent shear stress

Erythrocyte suspensions were exposed to constant shear stresses of 5-100 Pa with 10 Pa increments for 300 seconds. For intermittent shear exposure, couette cylindrical system was stopped repeatedly following a pre-determined time period (either 10 times of 30 seconds measurements, 10x30 sec, or 20 times of 15 seconds, 20x15 sec). Between each of the 10x30 or 20x15 sec shear stress period, 10 seconds of waiting durations were included. Each stress period was held at constant shear magnitude (i.e. 30 Pa).

2.5.2. Erythrocyte damage models

2.5.2.1. Oxidative stress model

Oxidative stress in vitro was generated using hydrogen peroxide (Sigma – Aldrich, H3410). Erythrocyte suspensions (5% Hct) were incubated with sodium azide (2mM) at 37^{o}C for 5 minutes prior to the peroxide addition. Hydrogen peroxide was added to the erythrocyte suspension at a final concentration of 1 mM and followed by 25 minutes of incubation at 37^{o}C. ıncubated suspensions were washed at least three times with isotonic PBS solutions at 3000 rpm for 5 minutes. Before the deformability measurements, previously washed erythrocytes were resuspended in PBS. Similar continuous shear stress was applied to these cells as control group.

2.5.2.2. Metabolic depletion

Similar experimental protocol of pre and post deformability measurements following the cell stability test was obtained only with the difference that this set of experiment included both the

fresh blood and the same blood after it was stored for 48h at room temperature. Measurements included both the 1st and the 3rd day. Same shear stress (5-100 Pa, 300 sec) range was applied following the deformability measurements. Before any shear stress was applied, deformability was recorded as well.

2.6. Data analysis

Before and after the preconditioning shear exposure, erythrocyte deformability was recorded. EI values obtained by the diffraction pattern analysis were plotted against shear stress. A sigmoidal curve was acquired as expected. EI-SS relationship was fitted by non-linear regression of Lineweaver Burk equation which provides information of (7): 1) Maximum elongation index (EI_{max}) at infinite stress; 2) the SS required to achieve one-half of this maximum deformation ($SS_{1/2}$). It is important to emphasize that deformability curve behaves atypically (i.e. at 100 Pa preconditioning) at the low regions of the curve, especially for lower values than 0.94 Pa. This might have been problematic while fitting the EI-SS curves; thus, the data were fitted for only those in the range of 1.65-50.0 Pa. Normalization of parameters obtained by non-linear regression analysis was provided by taking the ratio of $SS_{1/2}$ to EI_{max} to account for different extents of maximal deformation (7). Erythrocyte susceptibility to mechanical damage following preconditioning shear was evaluated by expressing the change in the ratio of $SS_{1/2}$ to EI_{max} corresponding to each preconditioning shear as a percentage regarding ratio of the control. Mechanical damage sensitivity can be calculated as follows:

$$\frac{\left(SS_{1/2} / EI_{\max_{pre-conditioned}}\right) - \left(SS_{1/2} / EI_{\max_{control}}\right)}{SS_{1/2} / EI_{\max_{control}}} \quad (3)$$

where $SS_{1/2}/EI_{max(preconditioned)}$ corresponded to $SS_{1/2}/EI_{max}$ measured after each preconditioning shear stress while $SS_{1/2}/EI_{max(control)}$ to $SS_{1/2}/EI_{max}$ measured before any preconditioning shear exposure (i.e. unsheared samples).

2.7. Statistical analysis

Results of either 10 (for healthy samples) or 5 (for damage models) experiments were recorded as mean ± standard error including various donors for each set. D'Agostino & Pearson omnibus normality test (Graphpad Software Inc, Release 5.0, USA) was used to test the normality of data. Each condition obtained from the data were compared with respect to one-way ANOVA as being repeated measurements; whether significant differences in means existed or not were checked (SPSS Inc, Release 19.0, USA). An alpha level of 0.05 was taken into account for determination of significance. Non-linear curve fitting was provided via Graphpad software to calculate $SS_{1/2}$ and EI_{max} parameters (Graphpad Software Inc, Release 5.0, USA). For oxidative stress and metabolic depletion

models, One-way ANOVA (for repeated measures) was used followed by Bonferoni post test with Graphpad software.

RESULTS

3.1. Hemogram results

Hemogram results were obtained for each donor to certify that all the donors were healthy and their blood parameters were in the normal range. For each set of experiments, hemogram results were calculated as mean ± standard deviation. Red blood cell count (RBC), hematocrit (HCT), mean corpuscular volume (MCV) and mean corpuscular hemoglobin concentration (MCHC) parameters were checked primarily. Mean ± standard deviation values for each set of experiments are calculated as follows:

Set of experiment	RBC ($10^3/mm^3$)	HCT (%)	MCV (μm^3)	MCHC(g/dl)
Sub-hemolytic threshold	5,2 ± 0,4	47,4 ± 4,3	90,8 ± 4,3	28,7 ± 0,6
Hydrogen peroxide treatment	5,1 ± 0,4	46,7 ± 5,8	91,3 ± 4,6	30,3 ± 0,7
Metabolic depletion	5,1 ± 0,8	49,2 ± 6,4	96,8 ± 5,0	30,4 ± 1,4

Table 3.1: Hemogram results of volunteers for each set of experiment. Mean ± standard deviation values of donors for each set of experiments

3.2. Erythrocyte morphology before mechanical stress exposure

The morphological examination of blood samples belonging to groups in Figure 3.1. is shown. These observations made with light microscopy, control and erythrocyte damage models did not differ morphologically. Microscopic images of erythrocytes after shear exposure could not be taken since erythrocyte samples were resuspended in viscous PVP prior to the shear measurements and it affected the image resolution.

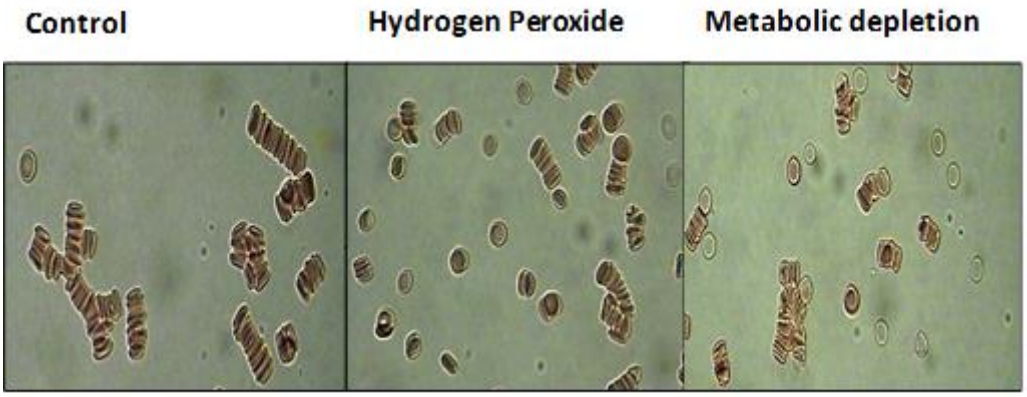

Figure 3.1: Microscopy images of erythrocytes obtained from subjects before (control) and after treatments of hydrogen peroxide and metabolic depletion, prior to SS exposure. RBCs are suspended in autologous plasma at low hematocrit (≈0.01 l/l)

3.3. Erythrocyte deformability responses to continuous shear stress

To ensure that the studies and results described below were not subject to artifacts due to hemolysis induced by SS exposure, a subset of bloods (n = 5) were employed to determine the concentration of free Hb in the PVP suspending media prior to and following application of SS (see Section 2.3).

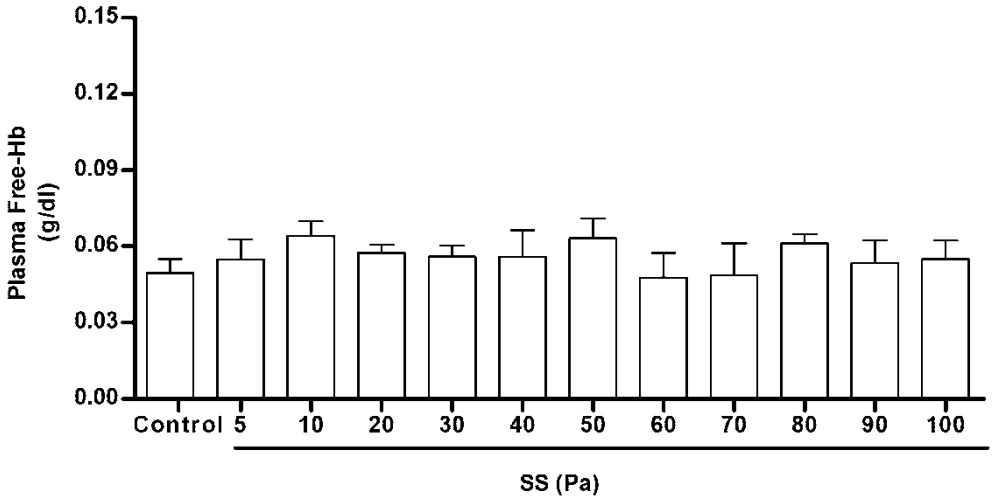

Figure 3.2: Plasma Free-Hemoglobin (16) measured at 300 s continuous exposure to shear stresses between 5 and 100 Pa. Data points are presented as mean ± standard error (n=5).

Over the SS range of 5 to 100 Pa and for an exposure time of 300 s, the free Hb was measured within the range of 0.05 to 0.06 g/dl while the Hb level in control sample was 0.05g/dl (representing only <0.1% hemolysis) (Figure 3.2.). Thus there was no detectable change compared to control ($p = 0.68$).

Red cell deformability was significantly influenced by 300 s of continuous exposure to shear stress (Figure 3.3.). The control (Con) curves were obtained for each donor using blood samples that were not previously exposed to SS; these data reflect the classic sigmoidal relationship between SS and EI. Following 300 s exposure to "physiological" SS (i.e., 5 and 20 Pa), EI as judged by the general positions of the curves, was not significantly changed compared with Con (Figure 3.3A). Note that more detailed analyses indicated improved deformability at 5 and 20 Pa (Figure 3).

When RBC were preconditioned at SS of 40 Pa or greater for 300 s, the EI at moderate-to-high SS was decreased when compared with Con (Figures 3.3.B and 3C) and the sigmoidal relationship between EI and SS was maintained only for stress >1.65 Pa. However, an "inflection" point was observed such that below this critical level, EI *increased* with decreasing SS: 0.5 Pa for 30

and 40 Pa preconditioned, 0.94 Pa for 50/60/70 Pa preconditioned and 1.65 Pa for 80/90/100 Pa preconditioned. In summary, the sigmoidal relationship was not maintained at lower SS when preconditioning was at 30 Pa or higher. Compared with control, preconditioning with 5-20 Pa for 300 s did not meaningfully change the EI-SS relationship (Figure 3.3.A), while at 30 Pa preconditioning, EI was significantly increased above control at 0.3 Pa ($p < 0.001$). Preconditioning at 40 Pa or greater for 300 s increased EI at 0.3 Pa ($p < 0.001$) and 0.53 Pa ($p < 0.05$) and significantly decreased EI at all SS between 1.65-16.0 Pa ($p < 0.001$).

Curve-fit parameters that describe EI-SS relations are presented in Figure 3.4., where it can be seen that preconditioning with 300 s of continuous 5-100 Pa SS did not alter EI_{max} (Figure 3.4.A). The SS required for half-maximal elongation index ($SS_{1/2}$) was, however, significantly influenced by exposure to 300 s of SS. While preconditioning at 5 and 20 Pa improved $SS_{1/2}$ (i.e., lower value and hence better deformability), preconditioning at 40 Pa and higher significantly increased $SS_{1/2}$ (Figure 3.4.B), indicating that greater stresses were required to achieve one-half of EI_{max}. When RBC deformability was expressed as the ratio of $SS_{1/2}$ divided by EI_{max}, similar results were observed: RBC deformability was improved by 300 s of continuous preconditioning at 5 Pa ($p < 0.001$) and 20 Pa ($p < 0.05$), whereas deformability was impaired by preconditioning at 40 Pa or greater ($p < 0.001$, Figure 3.4.C).

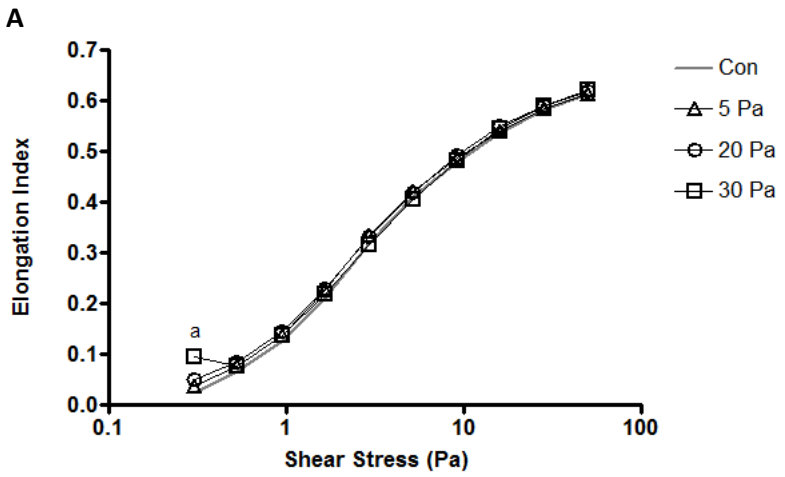

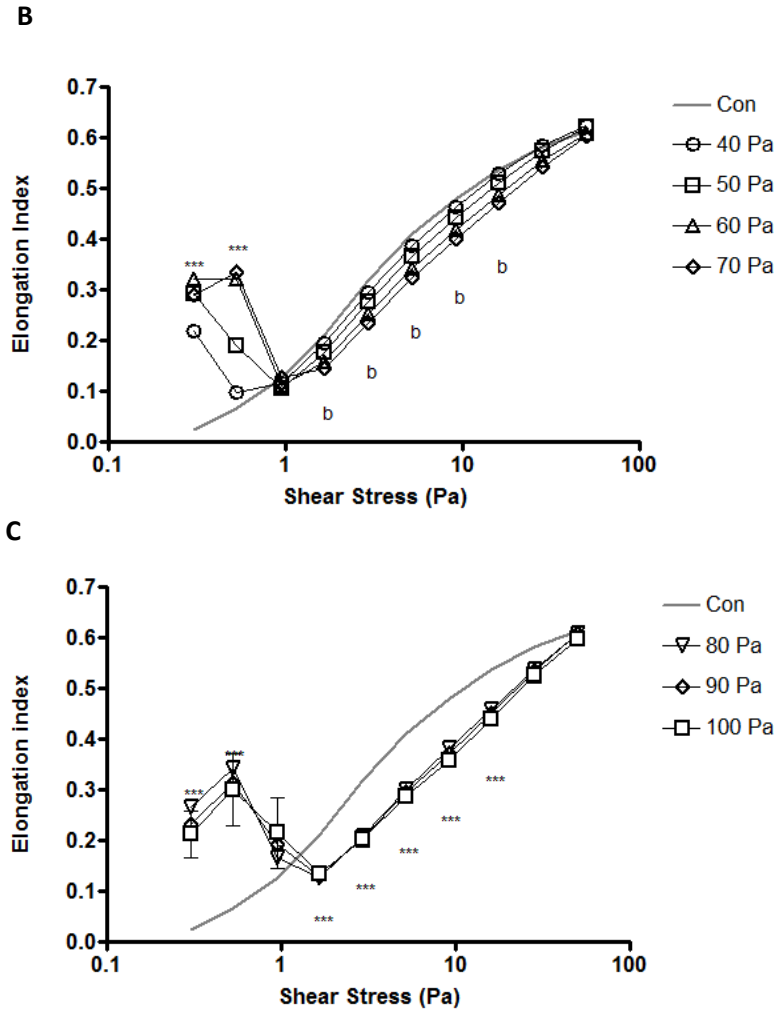

Figure 3.3: Elongation indexes (EI) measured at shear stresses between 0.3 and 50 Pa. Panel A presents EI-SS relations for RBC following 300 s continuous exposure to 5, 20 and 30 Pa SS. Panel B and C present the same relationships for RBC exposed for 300 s to 40-70 Pa and 80-100 Pa, respectively. Control (Con) data are for RBC that were not preconditioned. Data points are mean ± standard error (n=10), except Con is presented without symbols or error bars for clarity. Significant differences from Con ($p<0.001$): [a] = increase at 30 Pa; [b] = decrease at 60 and 70 Pa, *** = significantly different to Con.

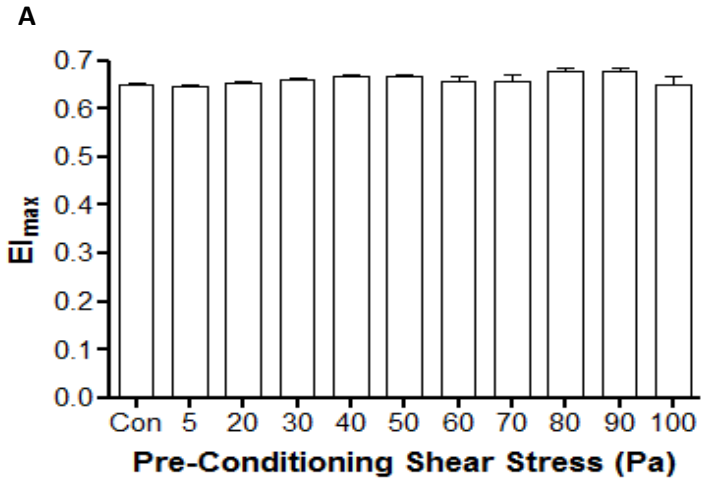

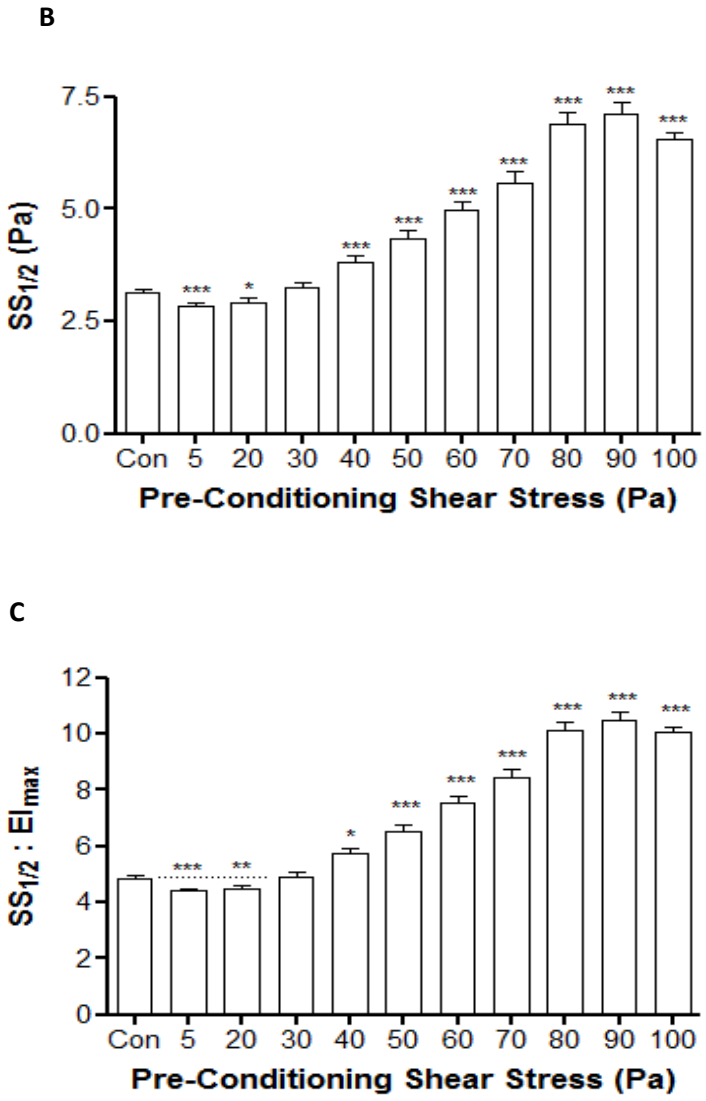

Figure 3.4: Curve-fit parameters that describe the elongation index-shear stress relationship for RBC exposed to 5-100 Pa for 300 s. Parameters shown are (panel A) maximal elongation index at infinite shear stress (EI_{max}), (panel B) the shear stress required for half-maximal deformation ($SS_{1/2}$), and (panel C) the ratio of $SS_{1/2}$ divided by EI_{max}. Control (Con) data were obtained for RBC that were not preconditioned. Data are mean ± standard error, n=10. ***, $p < 0.001$ significantly different from Con. **, $p < 0.01$ significantly different from Con. *, $p < 0.05$ significantly different from Con.

Individual donor sensitivity to SS (i.e., "mechanical damage sensitivity") is presented in Figure 3.5. Except for two donors (black square, black triangle), all other donors demonstrated improved RBC deformability (i.e., lower $SS_{1/2}$ and $SS_{1/2}/EI_{max}$) within the range of 5-20 Pa preconditioning. While preconditioning at 30 Pa resulted in an unaltered *mean* EI (i.e., unchanged deformability, Figures 3.5.B and 5C), individuals responses demonstrate that at least 30% (i.e., 3/10) of the donors (open circle, open triangle, open square) had improved RBC deformability at this SS. Moreover, one of these donors (open circles, Figure 3.5.) maintained 'normal' RBC deformability after 40 Pa preconditioning, while all other donors demonstrated damaged RBC at 40 Pa and greater SS.

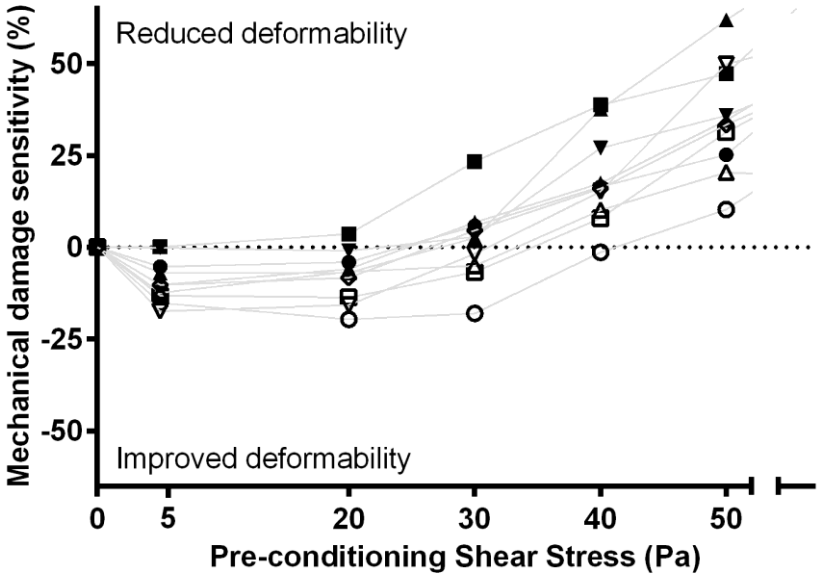

Figure 3.5: Individual donor sensitivity to shear stress (mechanical damage sensitivity) of red blood cells (RBC) expressed as percentage change of $SS_{1/2}/EI_{max}$ following preconditioning when compared with Control. RBC suspensions were subjected to 300 s of continuous shear stress at select stresses (5-100 Pa; only 5-50 Pa illustrated for clarity). Values < 0 represent increased (i.e., improved) RBC deformability, whereas values >0 represent decreased (i.e., reduced) RBC deformability. (n=10).

Elongation indexes change during the 300 s preconditioning period and represent the dynamic adjustment of RBC morphology during the application of SS; these data can be fit with an exponential curve to express the rate change of EI during SS exposure. From resting RBC morphology, RBC deform rapidly under SS application and reach a new "steady state" EI in a SS dependent manner; the time constant for this change is presented in Figure 3.6. The rate of change of RBC deformability was negatively and non-linearly related to the shear stress utilized during preconditioning, and hence preconditioning had a significant effect on the time constant ($F = 105$, $p < 0.001$). The rate of change of RBC deformability was significantly slower when preconditioning was at lower SS: preconditioning at 5 Pa resulted in RBC taking about 2-fold longer to change shape when compared with 10 Pa (5.0 ± 1.1 s vs. 2.3 ± 0.5 s; $p < 0.001$). A similar relative difference (~ 2-fold longer) was observed when comparing 10 Pa and 20 Pa preconditioning (2.3 ± 0.5 s vs. 0.98 ± 0.2 s; $p < 0.001$). Once RBC were exposed to ≥ 20 Pa SS, no further significant decrement in RBC deformability was observed, despite a non-significant trend ($p = 0.067$) being observed when comparing time constants at 20 Pa and 50 Pa.

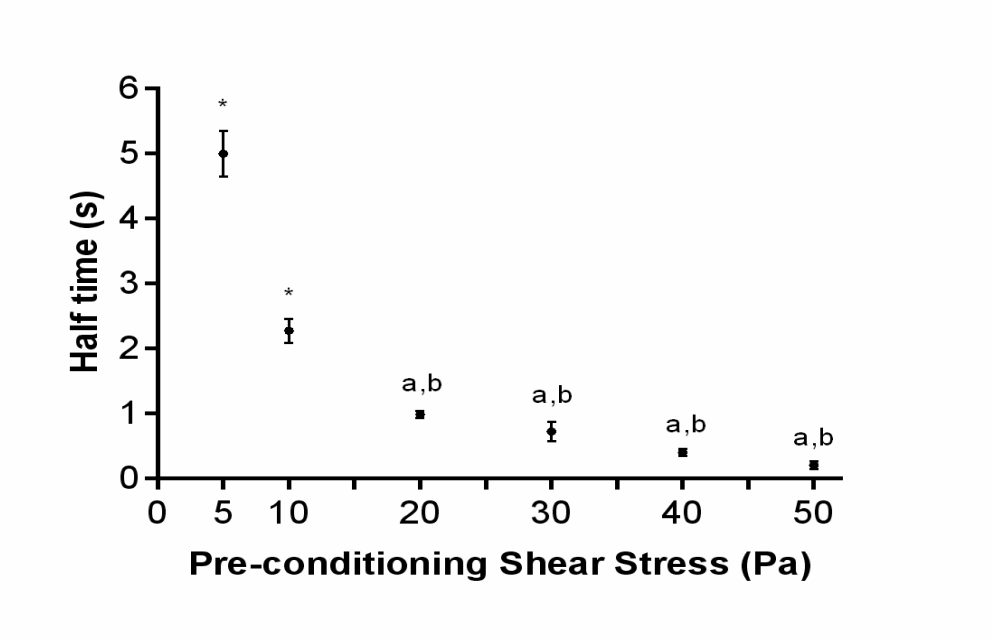

Figure 3.6: The time constant of the change in RBC deformation, which represents the half time (s) between resting RBC geometry and asymptotic elongation index, following the application of select SS (5-50 Pa) for 300 s. Values are mean ± SEM, n=10. [*], $p < 0.001$ significantly different from all other conditions. [a], significantly different from 5 Pa. [b], significantly different from 10 Pa.

3.4. Intermittent vs. continuous shear stress application

Elongation index-shear stress data for RBC exposed to continuous and intermittent applications of shear stress for 300 s are presented in Figure 6. Application of 10 Pa for 300 s increased EI at lower shears (i.e., 0.3–2.91 Pa) by 10-20% compared with control (all $p < 0.05$). This observation was consistent for all three conditions of SS application (1 x 300 s, 10 x 30 s, 20 x 15 s), and thus the 300 s application of 10 Pa increased the EI irrespective of whether SS was continuously or intermittently applied (Figure 3.7.A). When preconditioning was at 30 Pa (Figure 3.7.B), EI values were significantly increased at 0.3 Pa for all conditions ($p < 0.001$) and the 20 x 15 s preconditioning resulted in a significant increase in EI at 0.53 Pa ($p < 0.05$); no other differences were observed for 30 Pa preconditioning.

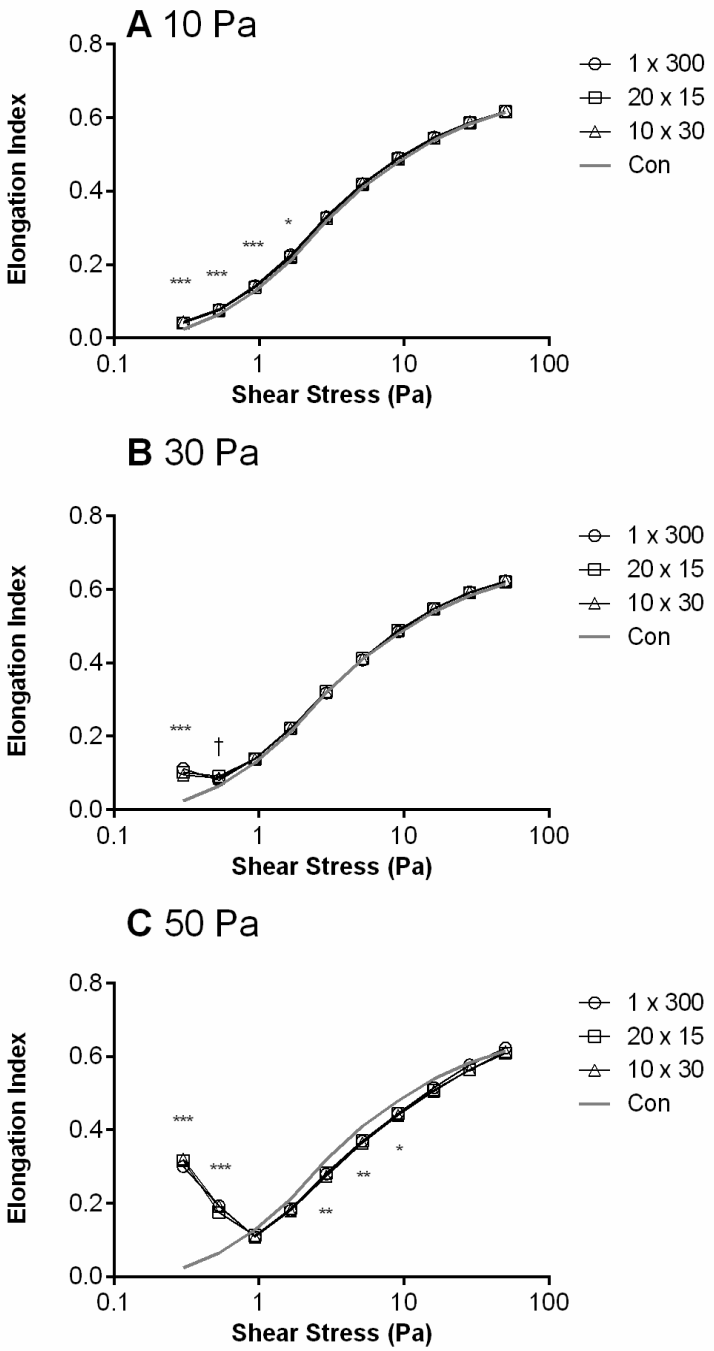

Figure 3.7: Elongation indexes measured at SS between 0.3 and 50 Pa for RBC exposed to 300 s of SS applied either continuously (1 x 300 s) or intermittently (20 times for 15 s each, 20 x 15; 10 times for 30 s each, 10 x 30). Experiments were conducted at 10 Pa (Panel A), 30 Pa (Panel B) and 50 Pa (Panel C). Control (Con) data were obtained for RBC that were not preconditioned. Data points are mean ± standard error, except Con is presented without symbols or error bars for clarity, n=10. ***, $p < 0.001$ all conditions different from Con. **, $p < 0.01$ all conditions different from Con. *, $p < 0.05$ all conditions different from Con. †, $p < 0.05$ 20 x 15 increased compared with Con.

The 50 Pa preconditioning markedly altered RBC deformability (Figure 3.7.C): EI was significantly increased at 0.3 and 0.53 Pa ($p < 0.001$) irrespective of whether preconditioning was applied continuously or intermittently. No differences in EI were observed at 0.91 and 1.65 Pa, but decreases were observed at 2.91 – 9.09 Pa inclusive, for both continuous and intermittent applications of SS (p range: < 0.01 to < 0.05).

Curve-fit parameterization of the EI-SS results presented in Figure 6 indicated that both intermittent and continuous applications of SS significantly influenced RBC deformability (Figure 3.8.). Preconditioning at 10 Pa resulted in a significantly decreased $SS_{1/2}/EI_{max}$ ratio and hence improved deformability when applied continuously for 300 s, and when applied intermittently 10 times for 30 s ($p < 0.05$); however, 20 applications of 15 s did not change this parameter (Figure 3.8.A). When RBC were exposed to 30 Pa of preconditioning, neither the continuous nor the intermittent protocols influenced $SS_{1/2}$:EI_{max} (Figure 3.8.B), whereas at 50 Pa $SS_{1/2}/EI_{max}$ was significantly increased (i.e., impaired deformability) for both intermittent and continuous protocols (Figure 3.8.C).

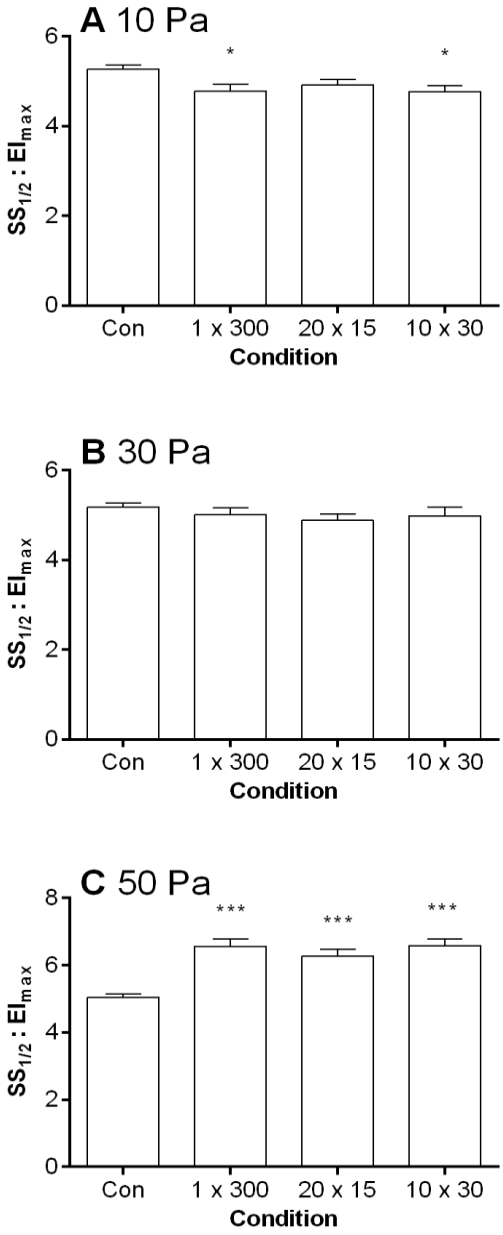

Figure 3.8: Curve-fit parameters that describe the elongation index-shear stress relationship for RBC suspensions exposed to 300 s of SS applied either continuously (1 x 300 s) or intermittently (20 x 15 s; 10 x 30 s). Experiments were conducted at 10 Pa (Panel A), 30 Pa (Panel B) and 50 Pa (Panel C). Control (Con) data were obtained in RBC that were not preconditioned to 300-s of SS. Data are mean ± standard error, n=10. ***, $p < 0.001$ significantly different from Con. **, $p < 0.01$ significantly different from Con. *, $p < 0.05$ significantly different from Con

3.5. Free Hb analysis of damage models

Any artifacts due to hemolysis were to be checked for the model (unhealthy) groups as well. For metabolic depletion model, free Hb concentration increased only for 90 and 100 Pa, while oxidative damage caused an increase for almost every preconditioning SS except Control sample (before any SS). Data were statistically tested and changes were recorded as significant ($P<0.05$) (Figure 3.9).

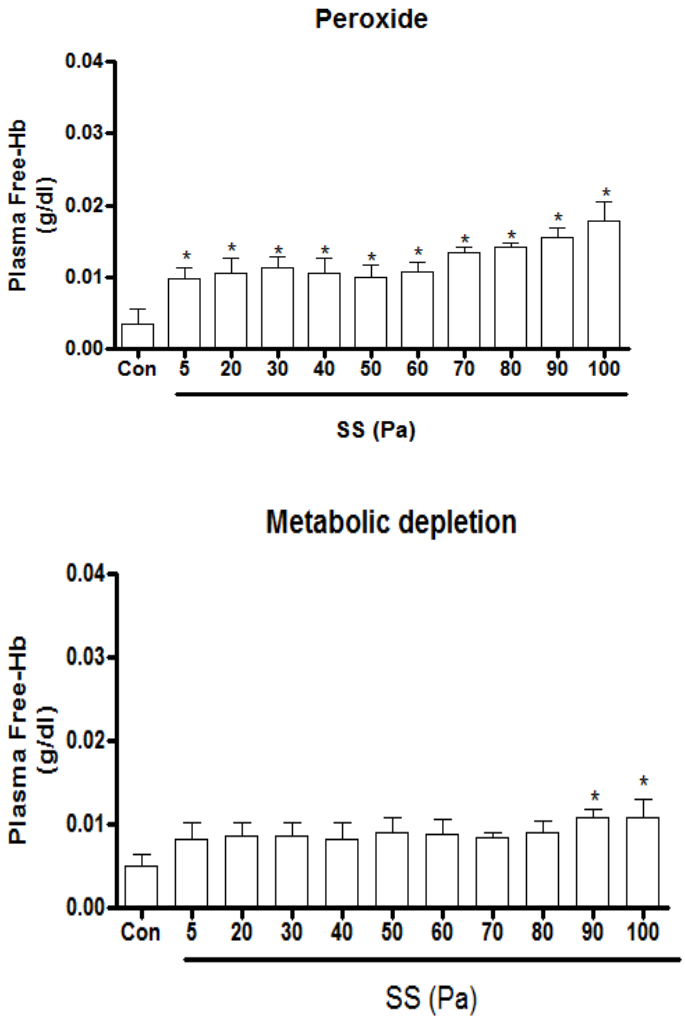

Figure 3.9: Free Hb concentration of oxidative stress and metabolic depletion model. Data represented as Mean±SEM

3.6. Erythrocyte deformability response to oxidative damage

Following the incubation with hydrogen peroxide, erythrocyte deformability was obviously impaired. Regular sigmoidal EI-SS relation for the peroxide treated cells was disrupted for supraphysiological SS values basically ($P<0.05$) and decreased deformability was obtained (Figure 3.10).

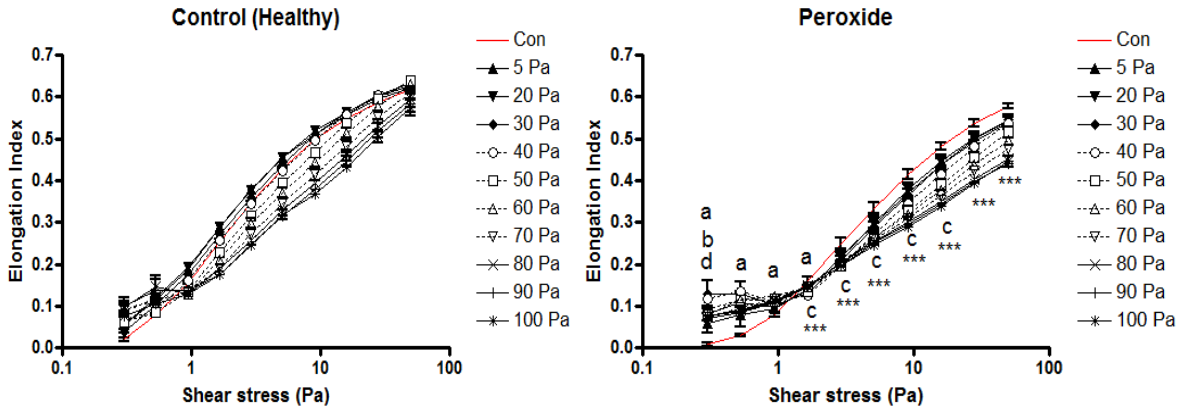

Figure 3.10: Elongation indexes (EI) measured at shear stresses between 0.3 and 50 Pa after hydrogen peroxide treatment. RBC suspensions were subjected to 300 s of continuous shear stress at select stresses (5-100 Pa). Control (Con) data are for RBC that were not preconditioned. Data points are mean ± standard error (n=5), except Con is presented without symbols or error bars for clarity. Significant differences from Con ($p<0.05$): [a] = increase at 5, 20 and 30 Pa; [b] = increase at 40, 50, 60 and 70 Pa, [c]= = decrease at 40, 50, 60 and 70 Pa, d= = increase at 80, 90 and 100 Pa *** = significantly different from Con at 80, 90 and 100 Pa SS. Left panel is placed here for viewing the trends between healthy and peroxide treated suspensions.

Preconditioning shear exposure of the oxidatively damaged samples at 30/40/50/100 Pa increased the deformability, which is slightly confusing. At 0.30 Pa of the EI-SS curve, preconditioning SS of 5/20/80/90/100 Pa increased the erythrocyte deformability. Between 0.53-1.65 Pa, increase in deformability at 5/20 Pa is seen from EI values. For the regions >1.65 Pa, significant decrease in erythrocyte deformability is seen at 40/50/60/70 Pa of preconditioning SS ($P<0.05$).

$SS_{1/2}$ and EI_{max} were calculated after obtaining the deformability measurements (Figure 3.11). Compared to Con values, EI_{max} values seemed to decrease significantly after oxidative damage for 5/40/50/60/70/80/90/100 Pa ($P<0.01$) and 20/30 Pa ($P<0.05$), respectively. The $SS_{1/2}$ values were significantly higher than untreated samples at 40/50 Pa of preconditioning SS ($P<0.01$) and at 30 Pa ($p<0.05$). Increased $SS_{1/2}$ was associated with decrease in the deformability. Increased $SS_{1/2}$ referred to higher SS values were required for the erythrocytes to reach one-half of EI_{max}. Preconditioning SS of 70 ($P<0.05$) and of 80/90/100 Pa ($P<0.01$) showed a decrease in $SS_{1/2}$ values compared to values corresponding to 5-50 Pa and the basic trend was biphasic but since the values are significantly higher than the Con, deformability kept decreasing at 100 Pa of preconditioning SS. Normalization of $SS_{1/2}$ by EI_{max} obtained similar results to that of $SS_{1/2}$ values only with changed significance levels. Preconditioning SS of 5/20/80/90 Pa decreased deformability ($p<0.05$) while SS values of 30/40/50/60/70/100 had a significance level of 0.01.

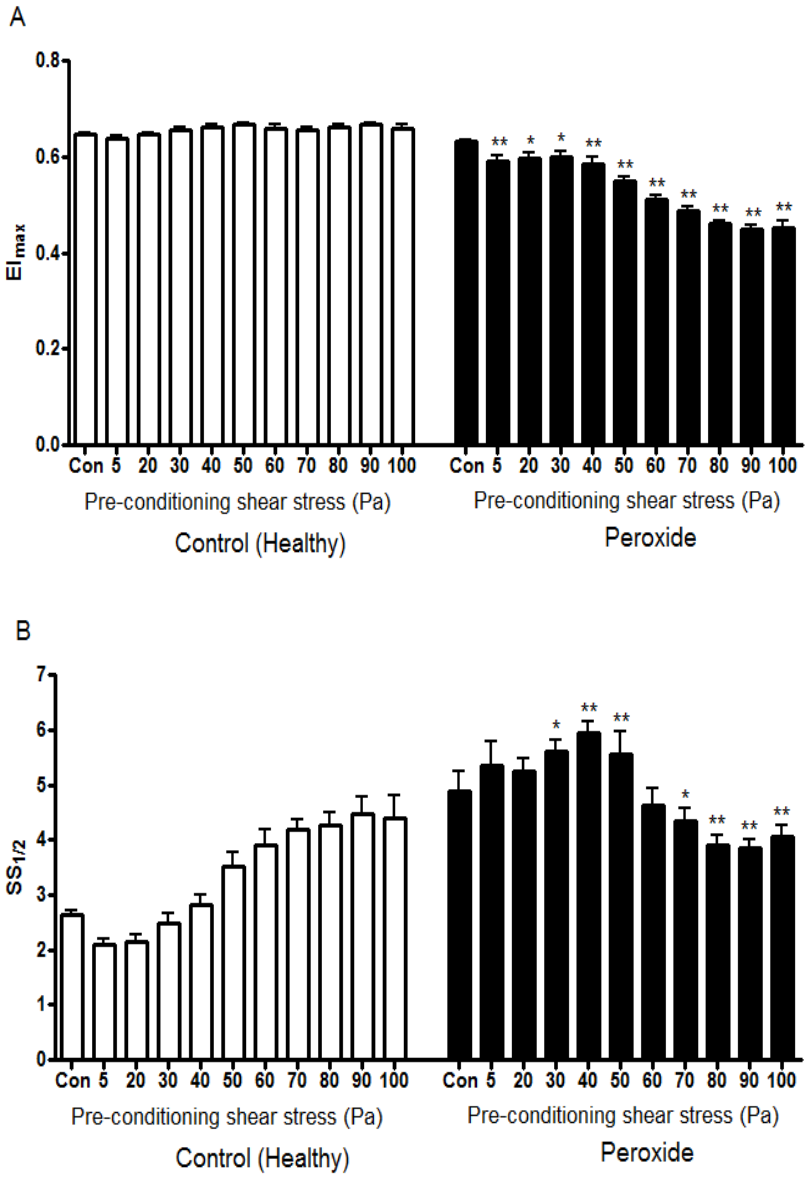
A
0.8
0.6
0.4
0.2
0.0
EImax
Con 5 20 30 40 50 60 70 80 90 100
Pre-conditioning shear stress (Pa)
Control (Healthy)
Con 5 20 30 40 50 60 70 80 90 100
Pre-conditioning shear stress (Pa)
Peroxide
B
7
6
5
4
3
2
1
0
SS1/2
Con 5 20 30 40 50 60 70 80 90 100
Pre-conditioning shear stress (Pa)
Control (Healthy)
Con 5 20 30 40 50 60 70 80 90 100
Pre-conditioning shear stress (Pa)
Peroxide

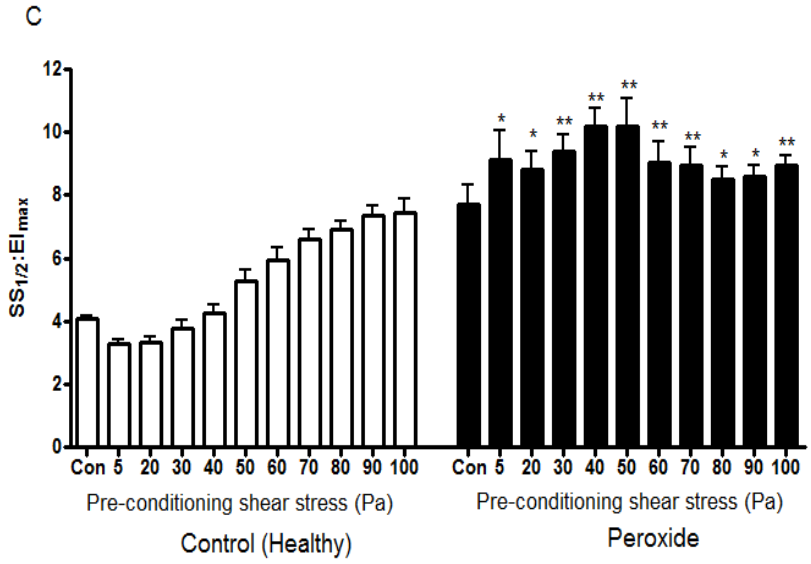

Figure 3.11: Curve-fit parameters that describe the elongation index-shear stress relationship for RBCs after hydrogen peroxide treatment exposed to 5-100 Pa for 300 s. Parameters shown are (panel A) maximal elongation index at infinite shear stress (EI_{max}), (panel B) the shear stress required for half-maximal deformation ($SS_{1/2}$), and (panel C) the ratio of $SS_{1/2}$ divided by EI_{max}. Control (Con) data were obtained for RBC that were not preconditioned. Data are mean ± standard error, n=5. **, $p < 0.01$ significantly different from Con. *, $p < 0.05$ significantly different from Con. Left panel is placed here for viewing the trends between healthy and peroxide treated suspensions.

Mechanical damage sensitivity shows the reduced deformability for peroxide treatment (Figure 3.12). Control group revealed expected results by for 5-20 Pa the mechanical damage sensitivity value was in the improved deformability range and for higher values, reduced deformability was recorded. On the contrary, after hydrogen peroxide treatment the mechanical damage sensitivity was in the reduced deformability region.

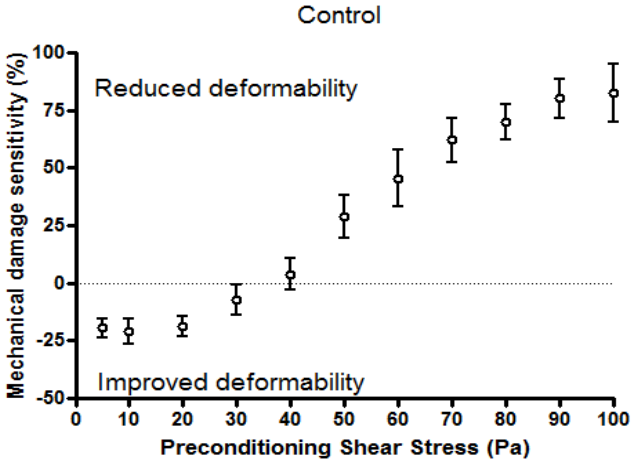

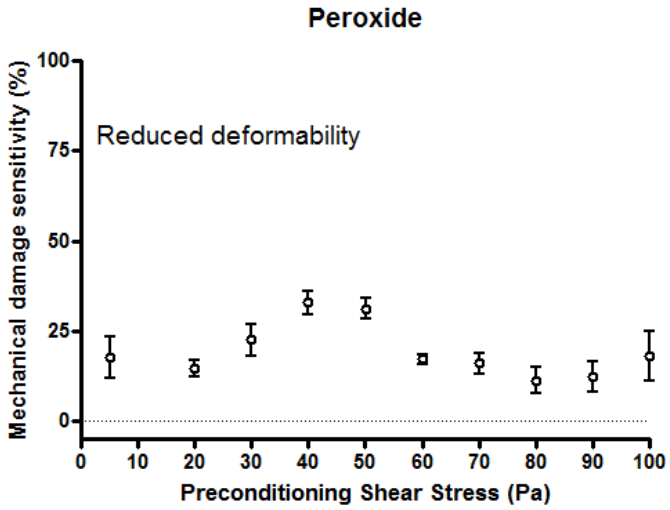

Figure 3.12: Mechanical damage sensitivity to shear stress of red blood cells (RBC) after hydrogen peroxide treatment expressed as percentage change of $SS_{1/2}/EI_{max}$ following preconditioning when compared with Control. RBC suspensions were subjected to 300 s of continuous shear stress at select stresses (5-100 Pa). Data are mean ± standard error, n=5. Values < 0 represent increased (i.e., improved) RBC deformability, whereas values >0 represent decreased (i.e., reduced) RBC deformability. (n=5). Upper panel is placed here for comparison healthy and peroxide treated suspensions.

3.7. Erythrocyte deformability response to metabolic depletion

The metabolic depletion model resulted in increased erythrocyte deformability after 48 hours. Regular sigmoidal EI-SS relation for both days was obtained and erythrocyte deformability decreased starting from 40 Pa of preconditioning SS both for the 1st and the 3rd day data (Figure 3.13).

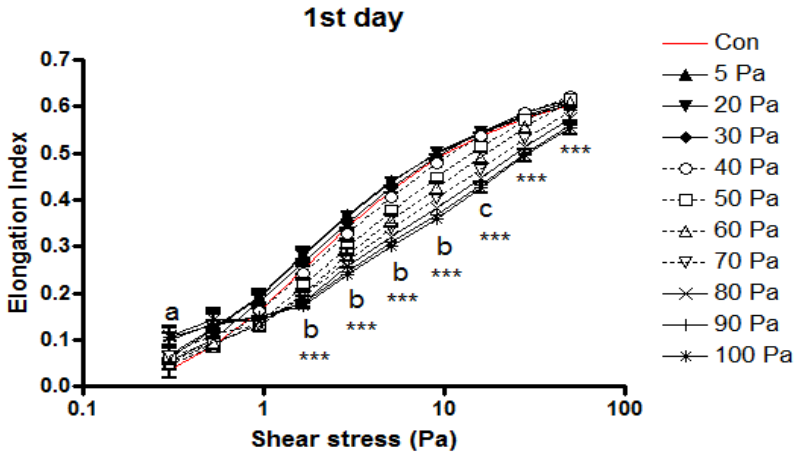

Figure 3.13: Elongation indexes (EI) measured at shear stresses between 0.3 and 50 Pa at first day metabolic depletion. RBC suspensions were subjected to 300 s of continuous shear stress at select stresses (5-100 Pa). Control (Con) data are for RBC that were not preconditioned. Data points are mean ± standard error (n=5), except Con is presented without symbols or error bars for clarity. Significant differences from Con ($p<0.05$): [a] = increase at 5 and 20 Pa; [b] = decrease at 50, 60, 70 and 80 Pa, [c]= = decrease at 70 and 80 Pa, *** = significantly different to Con at 80, 90 and 100 Pa SS.

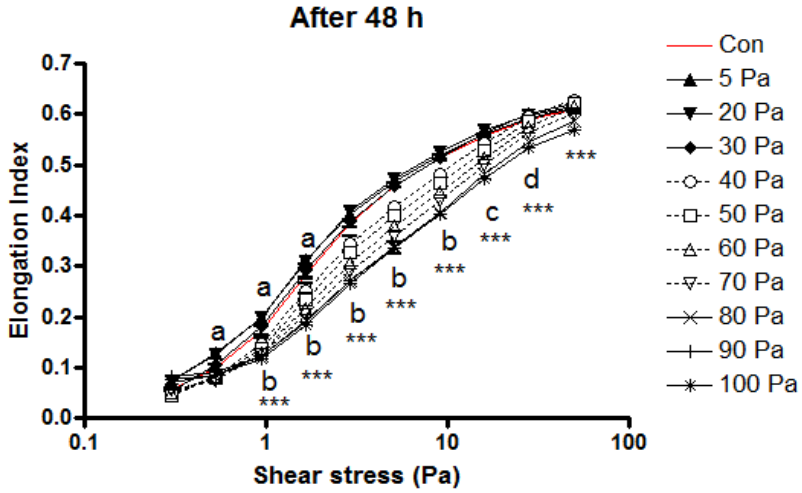

Fig 3.13 B: Elongation indexes (EI) measured at shear stresses between 0.3 and 50 Pa after 48 h metabolic depletion. Panel A presents EI-SS relations for erythrocytes following 300 s continuous exposure to shear stres. Control (Con) data are for RBC that were not preconditioned. Data points are mean ± standard error (n=5), except Con is presented without symbols or error bars for clarity. Significant differences from Con ($p<0.001$): [a] = increase at 5 and 20 Pa; [b] = decrease at 40, 50, 60 and 70 Pa, [c]= = decrease at 50, 60 and 70 Pa, d= = decrease at 70 Pa *** = significantly different to Con at 80, 90 and 100 Pa SS.

Preconditioning shear exposure of the samples corresponding to 48 hours after the blood was taken to 30/40/50/100 Pa increased the deformability. At <1.65 Pa of the EI-SS curve, preconditioning SS of 5/20 Pa significantly increased the erythrocyte deformability ($P<0.001$) compared to Con group (before any preconditioning SS). Significant decrease in deformability was recorded for preconditioning of 40/50/60/70 Pa in between 1.65-9.09 Pa of the EI-SS curve ($P<0.001$). Between 0.53-1.65 Pa, increase in deformability at 5/20 Pa is seen from EI values. For the regions >1.65 Pa, significant decrease in erythrocyte deformability is seen at 40/50/60/70 Pa of preconditioning SS ($P<0.05$). EI values at the region >9.09 Pa, significant decrease in erythrocyte deformability was observed for 50/60/70 Pa of preconditioning. From 50 Pa to 100 Pa of preconditioning SS, the significant change was observed compared to Con group, which was measured immediately after the blood was taken and without any preconditioning SS ($P<0.001$).

$SS_{1/2}$ and EI_{max} were obtained (Figure 3.14). Compared to Con values, EI_{max} values seemed to increase significantly at the 3rd day of metabolic depletion experiment for 90/100 Pa ($P<0.01$). The $SS_{1/2}$ values were significantly lower than data corresponding to the 1st day at 40/50/60/70/80/90/100 Pa of preconditioning SS ($P<0.01$). Decreased $SS_{1/2}$ was associated with decrease in the deformability. Decreased $SS_{1/2}$ meant that lower SS values were required for the erythrocytes to reach one-half of EI_{max}. Normalization of $SS_{1/2}$ by EImax obtained similar results to that of $SS_{1/2}$ values and data for 40-100 Pa of preconditioning SS of the 3rd day was significantly different than Con sample of the 1st day.

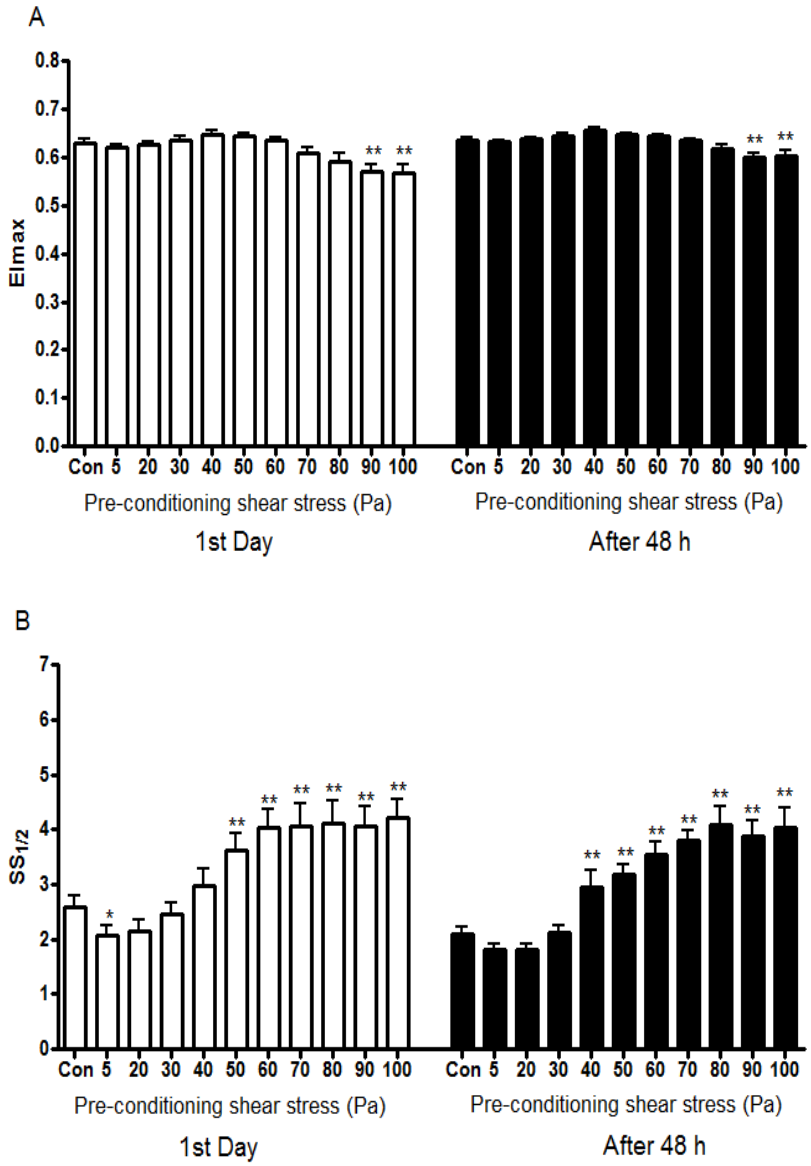
A
Elmax
0.8
0.7
0.6
0.5
0.4
0.3
0.2
0.1
0.0
Con 5 20 30 40 50 60 70 80 90 100
Pre-conditioning shear stress (Pa)
1st Day
Con 5 20 30 40 50 60 70 80 90 100
Pre-conditioning shear stress (Pa)
After 48 h
B
SS1/2
7
6
5
4
3
2
1
0
Con 5 20 30 40 50 60 70 80 90 100
Pre-conditioning shear stress (Pa)
1st Day
Con 5 20 30 40 50 60 70 80 90 100
Pre-conditioning shear stress (Pa)
After 48 h

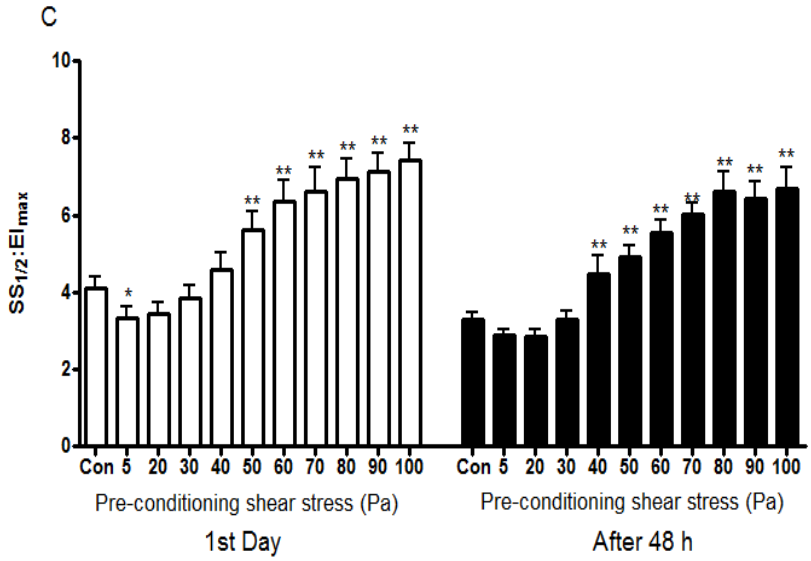

Figure 3.14: Curve-fit parameters that describe the elongation index-shear stress relationship for RBCs at first (A) and after 48 hours depletion exposed to 5-100 Pa for 300 s. Parameters shown are (panel A) maximal elongation index at infinite shear stress (EI_{max}), (panel B) the shear stress required for half-maximal deformation ($SS_{1/2}$), and (panel C) the ratio of $SS_{1/2}$ divided by EI_{max}. Control (Con) data were obtained for RBC that were not preconditioned. Data are mean ± standard error, n=5. **, $p < 0.01$ significantly different from Con. *, $p < 0.05$ significantly different from Con.

Mechanical damage sensitivity results show that for 5-20 Pa of preconditioning, deformability is improved while impairment was obtained for ≥ 40 Pa preconditioning shear stress both for the 1st and 3rd day of the metabolic depletion experiment. Trend of the curve is similar for both days (Figure 3.15).

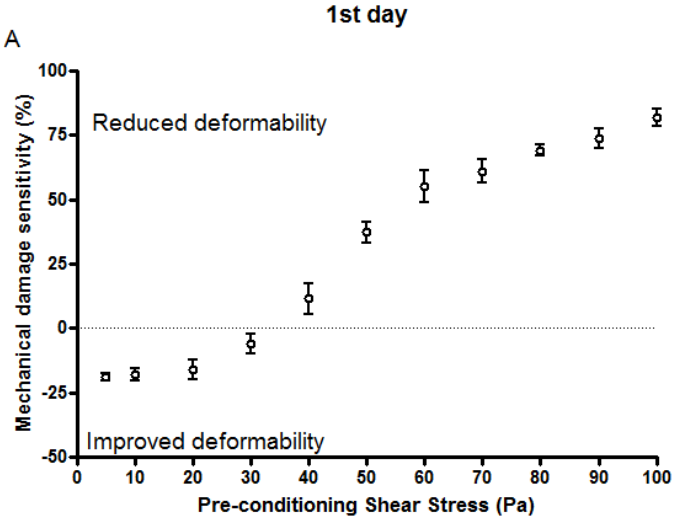

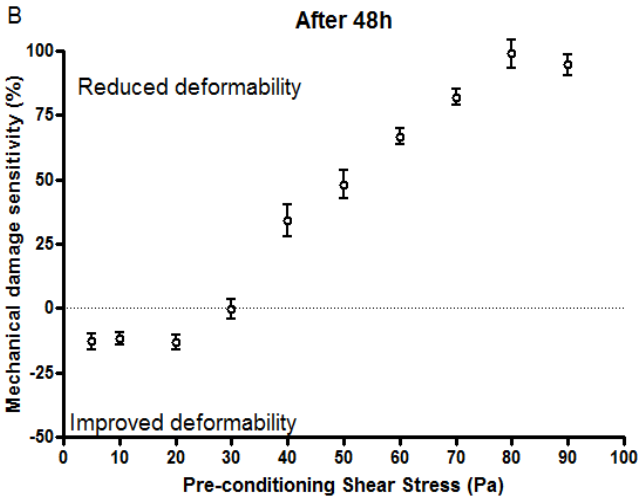

Figure 3.15: Mechanical damage sensitivity to shear stress of red blood cells (RBC) first (A) and after 48 hours (B) of metabolic depletion expressed as percentage change of $SS_{1/2}/EI_{max}$ following preconditioning when compared with Control. RBC suspensions were subjected to 300 s of continuous shear stress at select stresses (5-100 Pa). Data are mean ± standard error, n=5. Values < 0 represent increased (i.e., improved) RBC deformability, whereas values >0 represent decreased (i.e., reduced) RBC deformability. (n=5).

DISCUSSION

It was observed that 300 seconds of SS exposure may either improve or impair erythrocyte deformability depending on the magnitude of applied shear. Findings of this study are stated as:

i. When shear exposure was in the physiological range (5-20 Pa), shape of the EI-SS curves obtained from deformability measurements did not change although a decreased $SS_{1/2}$:EI_{max} was observed.

ii. Preconditioning RBC at supra-physiological SS was associated with "sub-hemolytic" damage; the first detection of sub-hemolytic damage was at 30 Pa preconditioning SS. The damage was obvious for ≥40 Pa preconditioning SS.

iii. When sub-hemolytic damage was present, an atypical deflection in the EI-SS curves were obtained at low shear regions of deformability curves.

iv. Regardless of being continuous or intermittent, 300 sec of shear exposure caused same sub-hemolytic damage. Intermittent conditions were either 10 times 30 (10x30 sec) or 20 times 15 (20x15 sec)of shear exposure.

v. The results were donor-specific regarding the tolerance to mechanical trauma.

vi. Erythrocyte damage models altered the erythrocyte deformability; oxidative damage model resulted in impairment while metabolic depletion yielded a slight increase.

vii. Subhemolytic threshold for metabolic depletion model shifted from 30 to 40 Pa at the 3rd day of the experiment.

From these findings, it can be concluded that when RBC are exposed to SS within the physiological range, no detectable damage is observed and the cells are possibly "primed" for improved deformation. However, when RBC are exposed to mildly supra-physiological SS (i.e., 30 Pa), RBCs tolerate this atypical exposure to stress and deformability at lower levels of SS was subsequently increased. These results might be considered as indicators for the capacity of circulatory system to tolerate mildly elevated SS within different regions of vasculature while showing possible limitations of traditional methods to detect mechanical damage.

A broad range of SS was employed in our study because physiologically, erythrocytes are exposed to different levels of SS while circulating in the vasculature. At vessels perfusing human eye, for instance, SS reaches to 15 Pa or more (48). It is known that within microvasculature, being a high shear region, transit time is relatively short. With laminar flowing arteries, on the other hand, the SS magnitude is in between 1 and 7 Pa (58). According to our results, continuous exposure to 5-20 Pa of SS, similar to that of *in vivo* conditions, improved erythrocyte deformability (Figure 3.4). Improvement in erythrocyte deformability following exposure to 5 and 20 Pa SS was also recorded in

the study of Meram et al (63). Their hypothesis was based on the fact that improvement in the erythrocyte deformability is associated with accumulation of regulatory products functioning for active regulation of erythrocyte deformability. Their findings proved that the improvement does not disappear for approximately 60 seconds after SS is removed. This study was not conducted in a biochemical aspect although previous studies indicate that the magnitude and duration of SS exposure influences adenosine triphosphate and NO release from RBC (101, 113); rather mechanical changes were analyzed regarding the magnitude and duration of the SS exposure.

NO is known to be one of the major agents regulating the erythrocyte deformability (108). Nitric oxide synthase (72) is mechanosensitive. With the role of NO on the active regulation of erythrocyte deformability, it is likely that the exposure of erythrocytes to physiological SS activates the NO synthesis mechanisms as well as increasing the availability of NO, which in turn increases erythrocyte deformability. It is interesting to note that we observed a decrease in the time required for RBC to deform with preconditioning at increased SS (Figure 3.6) with diminishing effect being observed beyond 20 Pa. Elevated rate of change in erythrocyte morphology and improved erythrocyte deformability is obtained with inclining SS as long as its magnitude is within the physiological range. For higher SS (30-100 Pa), however, rate of change in erythrocyte deformability does not increase but an irreversible damage dominates which should be considered as sub-hemolytic damage for this condition. There are two possibilities for such findings: Observations made regarding the erythrocyte deformability and regulation mechanisms might be analyzed by an entirely mechanical perspective or it may result either from an imbalance of intracellular substrates and products or disruption of biochemical function.

Effect of continuous SS on erythrocyte integrity, both within and above the physiological range has been investigated in several studies but intermittent exposure has not been thoroughly analyzed. Exposure of SS greater than 30 Pa for 300 seconds gradually decreased the EI although an increase is seen for ≤1 Pa for the deformability measurements. This trend represents an atypical observation (i.e., EI increasing with decreasing shear stress at lower levels of SS) which is an early sign of tumbling motion and thus mechanical damage because in normal conditions EI does decrease with increasing magnitude of SS. In one study, it was recorded that the number of damaged erythrocytes decreased when hemolytic SS was applied intermittently rather than in a continuous manner (66). This result might be counted as reduced rate of erythrocyte destruction. There is still erythrocyte damage however when the deformability values are compared to control group which is not exposed to any SS beforehand.

Our study was conducted to investigate the intermittent shear application effect on subhemolytic damage rather than the hemolytic damage. Our results coincided with the findings that early stage of damage was to be detected in between 30-40 Pa (Figure 3.8A and 3.8B). Therefore, for intermittent application of SS, magnitude of the shear was carefully chosen above and below this threshold. 50 Pa of preconditioning SS was found to decrease deformability and cause cell damage either continuously or intermittently (1x30 sec or 20x15 sec) (Figure 3.8). This finding, using ektacytometry to detect the cell damage, supports the micrograph findings of Mizunama and Sakai that intermittent SS results in RBC damage (66). However, our results did not find any difference between conditions, suggesting that while hemolysis is attenuated by intermittent SS, the sub-hemolytic threshold appears more "fixed" and less influenced by the frequency of SS application and more so by the total duration of application.

This study also showed for the first time, that intermittent SS, when applied at physiological range (i.e. 10 Pa), caused an increase in erythrocyte deformability. However, no statistical significance was recorded between the magnitudes of improvement following intermittent or continuous SS application (Figure 3.8). Interestingly, effect of 20x15 seconds of SS exposure altered the deformability less compared to 10x30 seconds of exposure or 1x300 seconds. Improvement of erythrocyte deformability was recorded with significant increase in EI at low shear regions (Figure 3.4B) although $SS_{1/2}$:EI_{max} ratio did not change significantly (i.e., 20 x 15 s vs control, Figure 3.8). This unusual finding probably highlights the way in which the curve-fit parameters are calculated, essentially providing a single value that describes the entire EI–SS curve (10). Moreover, it is not surprising that $SS_{1/2}$/EI_{max} was not decreased when compared with control, considering that the EI–SS data were remarkably similar at higher levels of SS (i.e., >3 Pa, Figure 3.3).

Our results are supported by the literature, that fragmentation of erythrocytes is seen exceeding a threshold with SS exposure (66). When fragmentation takes place, broken cytoskeletal composites bind to band 3 causing a reduction in plasma membrane surface area and this decreases the erythrocyte elasticity. Despite the damage, however, our spectrometry results prove that there is no hemolysis taking place so that one can only talk about the subhemolytic damage.

The present findings indicate that intermittent SS within the physiological range tends to increase RBC deformability, but no more so than a single application of SS when the application duration is constant. Experimental manipulations regarding erythrocyte deformability should be analyzed in order to associate the alterations with flow conditions to have a broader view of *in vivo* vasculature. Basically, improved erythrocyte deformability might be counted as a developed mechanism related to appropriate tissue perfusion.

Our results demonstrated that intermittent shear exposure increases the deformability as long as it is in the physiological range but only for a single SS application when duration is constant. This may refer to the active mechanosensitive mechanisms involved in active regulation which are:

i. Activated within 15 seconds.
ii. Not reversed completely after 6-8 seconds of stasis period which referred to the duration period.
iii. Not decreased within 300 seconds of SS exposure.

In fact, erythrocytes are not exposed to 5 min of continuous SS *in vivo*. Moreover, the active regulation of deformability is not lost within 300 seconds. A broader examination is needed to see whether products regarding the regulation mechanisms are more active during the beginning of exposure and/or at a steady state condition following a preconditioning SS exposure.

Deformability impairment recorded at 30-100 Pa for both intermittent and continuous SS in this study may reflect alterations in intracellular ion concentration and/or physical changes to the plasma membrane. It is known that increase in intracellular calcium concentration decreases the erythrocyte deformability (23) which may explain the rigidification of RBC preconditioned at higher SS. It is stated that when erythrocytes are exposed to 130 Pa of SS for 2 minutes, intracellular calcium concentration increases 50% (75). Mechanical trauma induced by such an exposure can be eliminated via Ca channel blockers. As well as the Ca channel blockers, NO donor has a diminishing effect on impairment of erythrocyte deformability (12). If no nitric oxide donor is available, potassium channel blocker may have similar effects against mechanical trauma. These examples support the importance of intracellular ion balance intracellular ion balance (particularly potassium) in maintaining the integrity of erythrocytes. Erythrocyte fragmentation is also seen when the threshold of SS is exceeded (66, 69, 104). Fragmentation mostly occurs when broken cytoskeletal attachments bind to Band 3 protein which reduces the surface area of plasma membrane (66). Despite the fragmentation, no free hemoglobin was detected which leads us to conclude that the damage was not hemolytic but rather a subhemolytic one during 300 sec exposure to SS less than 100 Pa.

After examination of continuous and intermittent shear exposure effect on erythrocyte deformability, erythrocyte damage models were considered. For control groups (untreated samples), the improvement in deformability was seen at 5-20 Pa while starting from 30 Pa the impairment started as expected (Figure 3.10 and 3.13; panels A).

Exposure to 300 sec of preconditioning SS altered the erythrocyte deformability in the damage models as well as the healthy (untreated) cells. Erythrocyte damage models resulted in impairment in erythrocyte deformability for oxidative damage model acquired by hydrogen peroxide treatment, while metabolic depletion model showed an increase in the in deformability. Sigmoidal relationship of EI-SS was preserved for the metabolic depletion. Peroxide treatment showed atypical deflections within the curve after 30 Pa of preconditioning SS.

In oxidative stress model, erythrocytes were incubated with hydrogen peroxide prior to the deformability measurements. Hydrogen peroxide causes crosslinking of spectrin and Hb (99). The crosslink takes place irreducibly between spectrin and hemoglobin in an oxidative manner. Alterations due to this crosslinking should be emphasized since spectrin is one of the pivotal molecules regarding the erythrocyte deformability. Echinocyte formation might be seen after the treatment (99). According to the findings of the study, however, echinocyte formation was not recorded. Deformability index is known to decrease with hydrogen peroxide treatment. Furthermore, reduction in the deformability is dose dependent (99).

These results match with our data reasonably although we have not studied the dose dependency of hydrogen peroxide. Erythrocyte deformability obviously diminished when cells were incubated with hydrogen peroxide.

Peroxide treatment significantly impaired the erythrocyte deformability. $SS_{1/2}$ values showed a biphasic response to increased preconditioning SS. But despite the decrease in $SS_{1/2}$ after 50 Pa of preconditioning SS, deformability was still significantly lower than that of Con, which was the untreated sample without any preconditioning SS (Figure 3.11). A significant increase ($P<0.05$) was detected in erythrocyte deformability at the region <1.65 Pa of EI-SS curve for 5/20/30 Pa of preconditioning SS (Figure 3.10) but this increase is only seen at the region which atypical deflections are seen; thus, increase in such regions are not usually considered as representative.

Free Hb results of hydrogen peroxide treatment revealed significant differences compared to the treated sample with peroxide but exposed to no preconditioning SS (Figure 3.9). This finding matched with the impaired deformability since free Hb concentration was obtained differently for the treated samples which were exposed to SS and hemolysis might have been present.

Mechanical damage sensitivity calculations show that after peroxide treatment, all preconditioning SS values yielded a reduced deformability. No data remained in the improved deformability region, even physiological ranges of 5-20 Pa. The reduction in deformability is basically due to increased membrane rigidity following the crosslink between spectrin and Hb which is

oxidatively induced. Shear modulus associated with the membrane rigidity was found to increase 20-fold in one study which can be correlated with our findings (36).

Metabolic depletion model resulted in increased deformability at the 3rd day. The regular EI-SS relationship was preserved. A surprising finding that atypical deflection at >1.65 Pa was not observed for the EI-SS curve of the 3rd day which may represent the improvement in erythrocyte deformability for high preconditioning SS such as 90 and 100 Pa.

Normalization of $SS_{1/2}$ to EI_{max} demonstrated the deformability change more apparent than $SS_{1/2}$ values alone; the decrease was observed more clearly. Starting from 40 Pa of preconditioning SS, change in the deformability was significant ($P<0.001$). Hemolysis data showed that the only change in free Hb concentration occurred at 90 and 100 Pa of preconditioning SS (Figure 3.9). Thus, one might speculate hemolysis took place only at 90 and 100 Pa. This finding is not sufficient to express the increase in the deformability for lower SS values (50-70 Pa) as no hemolysis was found to be present for such values. At the physiological circumstances, erythrocyte deformability was expected to impair after 48 hours of blood donation. Studies state, however, the impairments might not take place until the 1st week (14).

Calculation of the mechanical damage sensitivity demonstrated that subhemolytic threshold shifted from 40 Pa to 30 Pa for 3rd day compared to 1st day, respectively because for the 1st day, 30 Pa of preconditioning SS gave a result that was in the improved deformability region. At the 3rd day, on the other hand, the subhemolytic threshold was 30 Pa for average of 5 donors. Furthermore, data of 5-20 Pa of the 3rd day was closer to"0" which meant erythrocyte deformability was reduced slightly.

In the literature, metabolic depletion has been shown to impair erythrocyte deformability. Mostly, effect of blood storage on the mechanical and cellular alterations was studied. In one study for instance, hemorheological parameters were compared through 40 days of blood storage (14). Deformability indices, abnormal shape changes and hemolysis percentage were compared. This study has a coinciding part with our experiment. An improvement in deformability is seen within 28th day of storage as well as the 35th and 42nd days. The increase in deformability is partly explained by hemolysis; the percentage is notably high at the final days of storage. Therefore, it can be concluded that with hemolysis, the unhealthy cells are lysed whereas the healthy cells remain in the suspending media and yield relatively high deformability values. The mechanism behind reduced deformability remains unclear because there is said to be two possible mechanisms which might induce the reduction being either the oxidative mechanisms, gradually affecting the membrane skeleton via interactions between spectrin-actin, or progressive depletion of ATP. Significant alterations in shape and other hemorheological parameters were recorded starting from 2nd week of storage.

Generally, data obtained in the study are not fully applicable to *in vivo* conditions yet. The phenomena observed in the present study indicate, however, that RBC deformability is significantly improved following exposure to SS levels typical of those experienced in the human arterial circuit. It is therefore attractive to speculate that the pathways involved in the active regulation of RBC deformability may be "primed" within larger vessels (e.g., arteries) for improved microcirculatory transit. This hypothesis is indirectly supported by experimental models using suspensions with mildly decreased RBC deformability that indicated significantly increased flow resistance (104), longer RBC transit time (108), and redistribution of tissue hematocrit that ultimately disrupted tissue oxygen delivery (72). Models included oxidative damage by hydrogen peroxide and metabolic depletion. These two combine the chemical change within the erythrocyte membrane, its metabolism and the mechanical response, known as deformability. This study is expected to light up new insights regarding erythrocytes and vasculature because observing the *in vitro* changes for erythrocytes both in physiological and modified media will provide a strong contribution to speculate how erythrocytes behave *in vivo* in case of abnormalities or alterations.

BIBLIOGRAPHY

1. **Ami RB, Barshtein G, Zeltser D, Goldberg Y, Shapira I, Roth A, Keren G, Miller H, Prochorov V, Eldor A, Berliner S, and Yedgar S**. Parameters of red blood cell aggregation as correlates of the inflammatory state. *American journal of physiology Heart and circulatory physiology* 280: H1982-1988, 2001.
2. **Armstrong JK, Meiselman HJ, and Fisher TC**. Inhibition of red blood cell-induced platelet aggregation in whole blood by a nonionic surfactant, poloxamer 188 (RheothRx injection). *Thrombosis research* 79: 437-450, 1995.
3. **Arora D, Behr M, and Pasquali M**. A tensor-based measure for estimating blood damage. *Artificial organs* 28: 1002-1015, 2004.
4. **Baskurt OK**. In vivo correlates of altered blood rheology. *Biorheology* 45: 629-638, 2008.
5. **Baskurt OK, Gelmont D, and Meiselman HJ**. Red blood cell deformability in sepsis. *American journal of respiratory and critical care medicine* 157: 421-427, 1998.
6. **Baskurt OK, Hardeman MR, Rampling MW, and Meiselman HJ**. *Handbook of Hemorheology and Hemodynamics*. IOS, 2007.
7. **Baskurt OK, Hardeman MR, Uyuklu M, Ulker P, Cengiz M, Nemeth N, Shin S, Alexy T, and Meiselman HJ**. Parameterization of red blood cell elongation index--shear stress curves obtained by ektacytometry. *Scandinavian journal of clinical and laboratory investigation* 69: 777-788, 2009.
8. **Baskurt OK, and Meiselman HJ**. Blood rheology and hemodynamics. *Seminars in thrombosis and hemostasis* 29: 435-450, 2003.
9. **Baskurt OK, and Meiselman HJ**. Cellular Determinants of Low-Shear Blood Viscosity. *Biorheology* 34: 235-247, 1997.
10. **Baskurt OK, and Meiselman HJ**. Data reduction methods for ektacytometry in clinical hemorheology. *Clinical hemorheology and microcirculation* 54: 99-107, 2013.
11. **Baskurt OK, and Meiselman HJ**. Red blood cell mechanical stability test. *Clinical hemorheology and microcirculation* 55: 55-62, 2013.
12. **Baskurt OK, Uyuklu M, and Meiselman HJ**. Protection of erythrocytes from sub-hemolytic mechanical damage by nitric oxide mediated inhibition of potassium leakage. *Biorheology* 41: 79-89, 2004.
13. **Bateman RM, Jagger JE, Sharpe MD, Ellsworth ML, Mehta S, and Ellis CG**. Erythrocyte deformability is a nitric oxide-mediated factor in decreased capillary density during sepsis. *American journal of physiology Heart and circulatory physiology* 280: H2848-2856, 2001.
14. **Berezina TL, Zaets SB, Morgan C, Spillert CR, Kamiyama M, Spolarics Z, Deitch EA, and Machiedo GW**. Influence of storage on red blood cell rheological properties. *The Journal of surgical research* 102: 6-12, 2002.
15. **Bishop JJ, Nance PR, Popel AS, Intaglietta M, and Johnson PC**. Effect of erythrocyte aggregation on velocity profiles in venules. *American journal of physiology Heart and circulatory physiology* 280: H222–H236, 2001.
16. **Bize I, Guvenc B, Robb A, Buchbinder G, and Brugnara C**. Serine/threonine protein phosphatases and regulation of K-Cl cotransport in human erythrocytes. *The American journal of physiology* 277: C926-936, 1999.
17. **Boivin P**. Role of the phosphorylation of red blood cell membrane proteins. *The Biochemical journal* 256: 689-695, 1988.
18. **Bor-Kucukatay M, Wenby RB, Meiselman HJ, and Baskurt OK**. Effects of nitric oxide on red blood cell deformability. *American journal of physiology Heart and circulatory physiology* 284: H1577-1584, 2003.
19. **Bor-Kucukatay M, Yalcin O, Gokalp O, Kipmen-Korgun D, Yesilkaya A, Baykal A, Ispir M, Senturk UK, Kaputlu I, and Baskurt OK**. Red blood cell rheological alterations in hypertension induced by chronic inhibition of nitric oxide synthesis in rats. *Clinical hemorheology and microcirculation* 22: 267-275, 2000.

20. **Brown CH, 3rd, Lemuth RF, Hellums JD, Leverett LB, and Alfrey CP**. Response of human platelets to sheer stress. *Transactions - American Society for Artificial Internal Organs* 21: 35-39, 1975.
21. **Chasis JA, and Mohandas N**. Erythrocyte membrane deformability and stability: two distinct membrane properties that are independently regulated by skeletal protein associations. *The Journal of cell biology* 103: 343-350, 1986.
22. **Chien S**. Mechanotransduction and endothelial cell homeostasis: the wisdom of the cell. *American journal of physiology Heart and circulatory physiology* 292: H1209-1224, 2007.
23. **Chien S**. Red cell deformability and its relevance to blood flow. *Annual review of physiology* 49: 177-192, 1987.
24. **Davies PF**. Hemodynamic shear stress and the endothelium in cardiovascular pathophysiology. *Nature clinical practice Cardiovascular medicine* 6: 16-26, 2009.
25. **Day JR, and Taylor KM**. The systemic inflammatory response syndrome and cardiopulmonary bypass. *International journal of surgery* 3: 129-140, 2005.
26. **de Oliveira S, Silva-Herdade AS, and Saldanha C**. Modulation of erythrocyte deformability by PKC activity. *Clinical hemorheology and microcirculation* 39: 363-373, 2008.
27. **Deutsch S, Tarbell JM, Manning KB, Rosenberg G, and Fontaine AA**. Experimental fluid mechanics of pulsatile artificial blood pumps. *Ann Rev Fluid Mech* 38: 65-86, 2006.
28. **Dupire J, Socol M, and Viallat A**. Full dynamics of a red blood cell in shear flow. *Proceedings of the National Academy of Sciences of the United States of America* 109: 20808-20813, 2012.
29. **Edelman RR, and Manning WJ**. Magnetic resonance angiography and flow quantification of coronary arteries. *Magnetic resonance imaging clinics of North America* 1: 339-347, 1993.
30. **Fischer TM**. Tank-tread frequency of the red cell membrane: dependence on the viscosity of the suspending medium. *Biophysical journal* 93: 2553-2561, 2007.
31. **Fischer TM, and Korzeniewski R**. Effects of shear rate and suspending medium viscosity on elongation of red cells tank-treading in shear flow. *Cytometry Part A : the journal of the International Society for Analytical Cytology* 79: 946-951, 2011.
32. **Giersiepen M, Wurzinger LJ, Opitz R, and Reul H**. Estimation of shear stress-related blood damage in heart valve prostheses--in vitro comparison of 25 aortic valves. *The International journal of artificial organs* 13: 300-306, 1990.
33. **Gu YJ, Graaff R, de Hoog E, Veeger NJ, Panday G, Boonstra PW, and van Oeveren W**. Influence of hemodilution of plasma proteins on erythrocyte aggregability: an in vivo study in patients undergoing cardiopulmonary bypass. *Clinical hemorheology and microcirculation* 33: 95-107, 2005.
34. **H.H. L**. Shear stress in the circulation. In: *Flow-Dependent Regulation of Vascular Function*, edited by J.A. B, G K, and G.M. R. New York: Oxford University Press, 1995, p. 28–45.
35. **Halbhuber KJ, Feuerstein H, Stibenz D, and Linss W**. Membrane alteration during banking of red blood cells. *Biomedica biochimica acta* 42: S337-341, 1983.
36. **Hale JP, Winlove CP, and Petrov PG**. Effect of Hydroperoxides on Red Blood Cell Membrane Mechanical Properties. *Biophysical journal* 101: 1921–1929, 2011.
37. **Hartwell SK, and Grudpan K**. Flow-based systems for rapid and high-precision enzyme kinetics studies. *Journal of analytical methods in chemistry* 2012: 450716, 2012.
38. **Hebbel RP**. Beyond hemoglobin polymerization: the red blood cell membrane and sickle disease pathophysiology. *Blood* 77: 214-237, 1991.
39. **Heuser G, and Opitz R**. A Couette viscometer for short time shearing of blood. *Biorheology* 17: 17-24, 1980.
40. **Johnson RM**. Ektacytometry of Red Blood Cells. *Methods in Enzymology* 173: 35-54, 1989.
41. **Johnson RM, and Robinson J**. Morphological changes in asymmetric erythrocyte membranes induced by electrolytes. *Biochemical and biophysical research communications* 70: 925-931, 1976.
42. **Kamada T, McMillan DE, Sternlieb JJ, Bjork VO, and Otsuji S**. Albumin prevents erythrocyte crenation in patients undergoing extracorporeal circulation. *Scandinavian journal of thoracic and cardiovascular surgery* 22: 155-158, 1988.

43. **Kameneva MV, Watach MJ, Litwak P, Antaki JF, Butler KC, Thomas DC, Taylor LP, Borovetz HS, Kormos RL, and Griffith BP**. Chronic animal health assessment during axial ventricular assistance: importance of hemorheologic parameters. *ASAIO journal* 45: 183-188, 1999.
44. **Kassab GS**. Biomechanics of the cardiovascular system: the aorta as an illustratory example. *Journal of the Royal Society, Interface / the Royal Society* 3: 719-740, 2006.
45. **Kayar E**. İskemi - Reperfüzyon hasarın eritrosit mekaniğine etkisi. In: *Tıp Fakültesi Fizyoloji Anabilim Dalı*Akdeniz Üniversitesi, 1999, p. 1-63.
46. **Kodicek M, Suttnar J, Mircevova L, and Marik T**. Red blood cells under mechanical stress. *General physiology and biophysics* 9: 291-299, 1990.
47. **Korbut R, and Gryglewski RJ**. Nitric oxide from polymorphonuclear leukocytes modulates red blood cell deformability in vitro. *European journal of pharmacology* 234: 17-22, 1993.
48. **Koutsiaris AG, Tachmitzi SV, Batis N, Kotoula MG, Karabatsas CH, Tsironi E, and Chatzoulis DZ**. Volume flow and wall shear stress quantification in the human conjunctival capillaries and post-capillary venules in vivo. *Biorheology* 44: 375-386, 2007.
49. **Kusserow B, Larrow R, and Nichols J**. Metabolic and morphological alterations in leukocytes following prolonged blood pumping. *Transactions - American Society for Artificial Internal Organs* 15: 40-44, 1969.
50. **Kusserow BK, and Larrow R**. Studies of leukocyte response to prolonged blood pumping-effects upon phagocytic capability and total white cell count. *Transactions - American Society for Artificial Internal Organs* 14: 261-263, 1968.
51. **Lahet JJ, Lenfant F, Lecordier J, Bureau A, Duvillard L, Chaillot B, and Freysz M**. Effects of various osmolarity on human red blood cells in terms of potassium efflux and hemolysis induced by free radicals. *Biomed Pharmacother* 62: 697-700, 2008.
52. **Landis RC**. Redefining the systemic inflammatory response. *Seminars in cardiothoracic and vascular anesthesia* 13: 87-94, 2009.
53. **Lee SS, Antaki JF, Kameneva MV, Dobbe JG, Hardeman MR, Ahn KH, and Lee SJ**. Strain hardening of red blood cells by accumulated cyclic supraphysiological stress. *Artificial organs* 31: 80-86, 2007.
54. **Lehoux S, and Tedgui A**. Cellular mechanics and gene expression in blood vessels. *Journal of biomechanics* 36: 631-643, 2003.
55. **Leytin V, Allen DJ, Mykhaylov S, Mis L, Lyubimov EV, Garvey B, and Freedman J**. Pathologic high shear stress induces apoptosis events in human platelets. *Biochemical and biophysical research communications* 320: 303-310, 2004.
56. **Lipowsky HH, Kovalcheck S, and Zweifach BW**. The distribution of blood rheological parameters in the microvasculature of cat mesentery. *Circulation research* 43: 738-749, 1978.
57. **Loscalzo J**. Nitric oxide insufficiency, platelet activation, and arterial thrombosis. *Circulation research* 88: 756-762, 2001.
58. **Malek AM, Alper SL, and Izumo S**. Hemodynamic shear stress and its role in atherosclerosis. *JAMA : the journal of the American Medical Association* 282: 2035-2042, 1999.
59. **Manno S, Takakuwa Y, and Mohandas N**. Modulation of erythrocyte membrane mechanical function by protein 4.1 phosphorylation. *The Journal of biological chemistry* 280: 7581-7587, 2005.
60. **Marascalco PJ, Ritchie SP, Snyder TA, and Kameneva MV**. Development of standard tests to examine viscoelastic properties of blood of experimental animals for pediatric mechanical support device evaluation. *ASAIO journal* 52: 567-574, 2006.
61. **McBride WT, Armstrong MA, Crockard AD, McMurray TJ, and Rea JM**. Cytokine balance and immunosuppressive changes at cardiac surgery: contrasting response between patients and isolated CPB circuits. *British journal of anaesthesia* 75: 724-733, 1995.
62. **McKenna R, Bachmann F, Whittaker B, Gilson JR, and Weinberg M**. The hemostatic mechanism after open-heart surgery. II. Frequency of abnormal platelet functions during and after extracorporeal circulation. *The Journal of thoracic and cardiovascular surgery* 70: 298-308, 1975.
63. **Meram E, Yilmaz BD, Bas C, Atac N, Yalcin O, Meiselman HJ, and Baskurt OK**. Shear stress-induced improvement of red blood cell deformability. *Biorheology* 50: 165-176, 2013.

64. **Miller BE, and Levy JH**. The inflammatory response to cardiopulmonary bypass. *Journal of cardiothoracic and vascular anesthesia* 11: 355-366, 1997.
65. **Minamitani H, Tsukada K, Sekizuka E, and Oshio C**. Optical bioimaging: from living tissue to a single molecule: imaging and functional analysis of blood flow in organic microcirculation. *Journal of pharmacological sciences* 93: 227-233, 2003.
66. **Mizuno T, Tsukiya T, Taenaka Y, Tatsumi E, Nishinaka T, Ohnishi H, Oshikawa M, Sato K, Shioya K, Takewa Y, and Takano H**. Ultrastructural alterations in red blood cell membranes exposed to shear stress. *ASAIO journal* 48: 668-670, 2002.
67. **Mohandas N, and Chasis JA**. Red blood cell deformability, membrane material properties and shape: regulation by transmembrane, skeletal and cytosolic proteins and lipids. *Seminars in hematology* 30: 171-192, 1993.
68. **Mohandas N, Chasis JA, and Shohet SB**. The influence of membrane skeleton on red cell deformability, membrane material properties, and shape. *Seminars in hematology* 20: 225-242, 1983.
69. **Mohandas N, Clark MR, Health BP, Rossi M, Wolfe LC, Lux SE, and Shohet SB**. A technique to detect reduced mechanical stability of red cell membranes: relevance to elliptocytic disorders. *Blood* 59: 768-774, 1982.
70. **Mohandas N, and Gallagher PG**. Red cell membrane: past, present, and future. *Blood* 112: 3939-3948, 2008.
71. **Mohandas N, and Shohet SB**. The role of membrane-associated enzymes in regulation of erythrocyte shape and deformability. *Clinics in haematology* 10: 223-237, 1981.
72. **Naito K, Mizuguchi K, and Nose Y**. The need for standardizing the index of hemolysis. *Artificial organs* 18: 7-10, 1994.
73. **Nevaril CG, Lynch EC, Alfrey CP, Jr., and Hellums JD**. Erythrocyte damage and destruction induced by shearing stress. *The Journal of laboratory and clinical medicine* 71: 784-790, 1968.
74. **Ohno M, Hardeman MR, Dobbe JG, and Lettinga KP**. Laser assisted optical rotational cell analyzer (lorca). A new instrument for measurement of various structural hemorheological parameters. *Clinical hemorheology and microcirculation* 14: 606-618, 1994.
75. **Oonishi T, Sakashita K, and Uyesaka N**. Regulation of red blood cell filterability by Ca2+ influx and cAMP-mediated signaling pathways. *The American journal of physiology* 273: C1828-1834, 1997.
76. **Osterloh K, Gaehtgens P, and Pries AR**. Determination of microvascular flow pattern formation in vivo. *American journal of physiology Heart and circulatory physiology* 278: H1142-1152, 2000.
77. **Paszkowiak JJ, and Dardik A**. Arterial wall shear stress: observations from the bench to the bedside. *Vascular and endovascular surgery* 37: 47-57, 2003.
78. **Paul R, Apel J, Klaus S, Schugner F, Schwindke P, and Reul H**. Shear stress related blood damage in laminar couette flow. *Artificial organs* 27: 517-529, 2003.
79. **Pfafferott C, Meiselman HJ, and Hochstein P**. The effect of malonyldialdehyde on erythrocyte deformability. *Blood* 59: 12-15, 1982.
80. **Piagnerelli M, Boudjeltia KZ, Vanhaeverbeek M, and Vincent JL**. Red blood cell rheology in sepsis. *Intensive care medicine* 29: 1052-1061, 2003.
81. **Pries AR, and Secomb TW**. Control of blood vessel structure: insights from theoretical models. *American journal of physiology Heart and circulatory physiology* 288: H1010–H1015, 2005.
82. **Quinlan NJ, and Dooley PN**. Models of flow-induced loading on blood cells in laminar and turbulent flow, with application to cardiovascular device flow. *Annals of biomedical engineering* 35: 1347-1356, 2007.
83. **Rabinovitz RS, and Nerem RM**. Effects of branching angle in the left main coronary bifurcation. *Circulation* 4: 157-167, 1976.
84. **Reneman RS, Arts T, and Hoeks AP**. Wall shear stress--an important determinant of endothelial cell function and structure--in the arterial system in vivo. Discrepancies with theory. *Journal of vascular research* 43: 251-269, 2006.

85. **Reneman RS, Arts T, and Hoeks AP**. Wall Shear Stress – an Important Determinant of Endothelial Cell Function and Structure – in the Arterial System in vivo. *Journal of vascular research* 43: 251–269, 2006.
86. **Resnick N, Yahav H, Shay-Salit A, Shushy M, Schubert S, Zilberman LC, and Wofovitz E**. Fluid shear stress and the vascular endothelium: for better and for worse. *Progress in biophysics and molecular biology* 81: 177-199, 2003.
87. **Roberts D, Dernevik L, Hirayama T, Yamaguchi H, Allers M, and Williamolsson G**. Reduced Peroperative and Postoperative Mortality Following the Use of Urea during Elective Cardiopulmonary Bypass - a Proposed Treatment for the Prevention of Reduced Red-Cell Deformability during Open-Heart-Surgery. *J Cardiovasc Surg* 28: 75-80, 1987.
88. **Rother RP, Bell L, Hillmen P, and Gladwin MT**. The clinical sequelae of intravascular hemolysis and extracellular plasma hemoglobin: a novel mechanism of human disease. *JAMA : the journal of the American Medical Association* 293: 1653-1662, 2005.
89. **Rothlein R, Kishimoto TK, and Mainolfi E**. Cross-linking of ICAM-1 induces co-signaling of an oxidative burst from mononuclear leukocytes. *Journal of immunology* 152: 2488-2495, 1994.
90. **Royston D**. The inflammatory response and extracorporeal circulation. *Journal of cardiothoracic and vascular anesthesia* 11: 341-354, 1997.
91. **Seiyama A, Suzuki Y, Tateishi N, and Maeda N**. Viscous properties of partially hemolyzed erythrocyte suspension. *Biorheology* 28: 452, 1991.
92. **Shaaban AM, and Duerinckx AJ**. Wall shear stress and early atherosclerosis: a review. *AJR American journal of roentgenology* 174: 1657-1665, 2000.
93. **Shappell SB, Toman C, Anderson DC, Taylor AA, Entman ML, and Smith CW**. Mac-1 (CD11b/CD18) mediates adherence-dependent hydrogen peroxide production by human and canine neutrophils. *Journal of immunology* 144: 2702-2711, 1990.
94. **Sheetz MP**. Membrane skeletal dynamics: role in modulation of red cell deformability, mobility of transmembrane proteins, and shape. *Seminars in hematology* 20: 175-188, 1983.
95. **Simchon S, Jan KM, and Chien S**. Influence of reduced red cell deformability on regional blood flow. *The American journal of physiology* 253: H898-903, 1987.
96. **Simmonds MJ, Meiselman HJ, and Baskurt OK**. Blood rheology and aging. *Journal of geriatric cardiology : JGC* 10: 291-301, 2013.
97. **Sirs JA**. The flow of human blood through capillary tubes. *The Journal of physiology* 442: 569-583, 1991.
98. **Snyder LM, Fortier NL, Trainor J, Jacobs J, Leb L, Lubin B, Chiu D, Shohet S, and Mohandas N**. Effect of hydrogen peroxide exposure on normal human erythrocyte deformability, morphology, surface characteristics, and spectrin-hemoglobin cross-linking. *The Journal of clinical investigation* 76: 1971-1977, 1985.
99. **Snyder LM, Fortier NL, Trainor J, Jacobs J, Lob L, Lubin B, Chiu D, Shohet S, and Mohandas N**. Effect of Hydrogen Peroxide Exposure on Normal Human Erythrocyte Deformability, Morphology, Surface Characteristics and Spectrin-Hemoglobin Cross-linking. *J Clin Invest* 76: 1971-1977, 1985.
100. **Sprague B, Chesler NC, and Magness RR**. Shear stress regulation of nitric oxide production in uterine and placental artery endothelial cells: experimental studies and hemodynamic models of shear stresses on endothelial cells. *The International journal of developmental biology* 54: 331-339, 2010.
101. **Sprague RS, Ellsworth ML, Stephenson AH, Kleinhenz ME, and Lonigro AJ**. Deformation-induced ATP release from red blood cells requires CFTR activity. *The American journal of physiology* 275: H1726-1732, 1998.
102. **Sumpelmann R, Schurholz T, Marx G, and Zander R**. Protective effects of plasma replacement fluids on erythrocytes exposed to mechanical stress. *Anaesthesia* 55: 976-979, 2000.
103. **Sutera SP**. Flow-induced trauma to blood cells. *Circulation research* 41: 2-8, 1977.
104. **Sutera SP, and Mehrjardi MH**. Deformation and fragmentation of human red blood cells in turbulent shear flow. *Biophysical journal* 15: 1-10, 1975.

105. **Tomaiuolo G, and Guido S**. Start-up shape dynamics of red blood cells in microcapillary flow. *Microvascular research* 82: 35-41, 2011.
106. **Toptas B, Baykal A, Yesilipek A, Isbir M, Kupesiz A, Yalcin O, and Baskurt OK**. L-carnitine deficiency and red blood cell mechanical impairment in beta-thalassemia major. *Clinical hemorheology and microcirculation* 35: 349-357, 2006.
107. **Tran-Son-Tay R, Sutera SP, Zahalak GI, and Rao PR**. Membrane stress and internal pressure in a red blood cell freely suspended in a shear flow. *Biophysical journal* 51: 915-924, 1987.
108. **Ulker P, Yaras N, Yalcin O, Celik-Ozenci C, Johnson PC, Meiselman HJ, and Baskurt OK**. Shear stress activation of nitric oxide synthase and increased nitric oxide levels in human red blood cells. *Nitric oxide : biology and chemistry / official journal of the Nitric Oxide Society* 24: 184-191, 2011.
109. **Untariou A, Wood HG, Allaire PE, Throckmorton AL, Day S, Patel SM, Ellman P, Tribble C, and Olsen DB**. Computational Design and Experimental Testing of a Novel Axial Flow LVAD. *ASAIO journal* 2005.
110. **V. KM, and F. AJ**. Mechanical trauma to blood. In: *Handbook of Hemorheology and Hemodynamics*, edited by K. BO, R. HM, W. RM, and H.J. M. Amsterdam, Netherlands: IOS Press, 2007, p. 206-227.
111. **Wachtfogel YT, Kucich U, Greenplate J, Gluszko P, Abrams W, Weinbaum G, Wenger RK, Rucinski B, Niewiarowski S, Edmunds LH, Jr., and et al.** Human neutrophil degranulation during extracorporeal circulation. *Blood* 69: 324-330, 1987.
112. **Wan J, Forsyth AM, and Stone HA**. Red blood cell dynamics: from cell deformation to ATP release. *Integrative biology : quantitative biosciences from nano to macro* 3: 972-981, 2011.
113. **Wan J, Ristenpart WD, and Stone HA**. Dynamics of shear-induced ATP release from red blood cells. *Proceedings of the National Academy of Sciences of the United States of America* 105: 16432-16437, 2008.
114. **Weed RI**. The importance of erythrocyte deformability. *The American journal of medicine* 49: 147-150, 1970.
115. **Wells R, and Goldstone J**. Rheology of red cell and capillary blood flow. In: *Rheology of biological systems*, edited by Gabelnick HL, and Litt MSpringfield, 1973, p. 5-11.
116. **Wurzinger LJ, Blasberg P, and Schmid-Schonbein H**. Towards a concept of thrombosis in accelerated flow: rheology, fluid dynamics, and biochemistry. *Biorheology* 22: 437-450, 1985.
117. **Yalcin O, Ulker P, Yavuzer U, Meiselman HJ, and Baskurt OK**. Nitric oxide generation by endothelial cells exposed to shear stress in glass tubes perfused with red blood cell suspensions: role of aggregation. *American journal of physiology Heart and circulatory physiology* 294: H2098-2105, 2008.
118. **Zheng Y, Nguyen J, Wang C, and Sun Y**. Electrical measurement of red blood cell deformability on a microfluidic device. *Lab on a chip* 13: 3275-3283, 2013.